B U L G A R I A N A C A D E M Y O F S C I E N C E S

INSTITUE OF ROBOTICS

Bulgaria, Sofia 1113, ZIP code 79, “Acad. G. Bonchev” str, Bl.2,

Phone.(+359 2) 8703361, 4053055, Fax: (+359 2) 4053061

An honorary member of "Council of the European Scientific and Cultural Community"

MEng. Svetoslav Emilov Kremenski

Integration of brain-machine interface and social robots with application in various object domains

Abstract

Of

Dissertation

Academic supervisors:

Prof. Anna Kostadinova Lekova – Institute of Robotics-BAS and

Prof. Snezhanka Kostova – Institute of Robotics-BAS

2026, Sofia

The dissertation thesis was discussed and admitted to defense by the Scientific Jury at an expanded meeting of the Interactive Robotics and Control Systems (IRCS) Section at the Institute of Robotics of the Bulgarian Academy of Sciences (BAS), held on April 24, 2026, by order of the Director No. 45/April 16, 2026.

The research for the dissertation was conducted at the Institute of Robotics - BAS.

The thesis has a total length of 177 pages and includes: an Introduction, Four Chapters, a Conclusion, Directions for future work, Scientific Contributions of the Dissertation, References, three Appendices, 35 figures, and 2 tables.

The defense materials are available at the office of the Institute of Robotics - BAS, Block 2, Room 406..

Author: MEng**. Svetoslav Emilov Kremenski**

Title: „**INTEGRATION OF BRAIN-MACHINE INTERFACE AND SOCIAL ROBOTS WITH APPLICATION IN VARIOUS OBJECT DOMAINS**"

Scientific Jury:

Internal members:

1. Prof. Maya Dimitrova
2. Prof. Tanyo Tanev

External members:

1. Prof. D.Eng. Daniela Borisova - IICT
2. Prof. D.Eng. Ivan Garvanov - ULSIT
3. Prof. George Popov – TU Sofia

I. General characteristics of the dissertation

The research domain of this doctoral dissertation focuses on Brain-Computer Interfaces (BCI), also referred to in literature as Brain-Machine Interfaces (BMI) and the methodologies for integrating them with social robots within the Internet of Things (IoT) ecosystem. This integration aims to expand traditional Human-Robot Interaction (HRI) across various domains, including education, customer service, healthcare, social integration, rehabilitation, and smart homes.The object of the research is the systemic combination of BCI technologies and social robotics within IoT frameworks. The subject of the research is the specific process of integration between BCIs and social robots within the IoT, aimed at optimizing and enhancing their communication and interaction. Driven by advancements in cloud computing, Artificial Intelligence (AI), and the IoT, BCI devices and social robots are projected to see widespread deployment, becoming ubiquitous in elderly care and personal assistance. Operating these billions of interconnected devices across smart homes, hospitals, and workplaces currently requires advanced multi-language programming skills or the utilization of visual programming tools. Visual programming addresses this complexity by logically decomposing intricate processes into simpler, modular micro-processes, thereby enabling custom scenarios tailored to specific user needs. A core component of this BCI-social robot integration involves investigating neural signal processing algorithms, which form the bedrock of BCI functionality by translating brain electrical activity into actionable machine commands. Furthermore, this research examines the specific approaches social robots utilize to interpret these neural signals, ensuring accurate, context-aware responses to BCI-initiated communication. This aspect is critical for social robots deployed in sensitive, high-interaction environments such as eldercare, education, and assistive technologies for individuals with disabilities.

Relevance of the problem

According to global management consulting and market research firms such as IMARC Group and Grand View Research, the combined market for Brain-Computer Interface (BCI) devices and robotics—including social robots—is projected to scale to billions of interconnected units by 2030. This forecast aligns with the rapid expansion trends observed in both sectors, catalyzed by breakthroughs in Artificial Intelligence (AI), neurotechnology, and robotics.Data from Grand View Research indicates that the global BCI market is poised for significant expansion, with valuations expected to rise from $1.74 billion in 2022 to $6.2 billion by 2030. The primary drivers for this growth reside in healthcare, retail, gaming, and smart home environments. Concurrently, robotics technologies (encompassing humanoid, social, and collaborative robots) continue to advance across key sectors such as clinical care, education, and assistive technology. Consequently, users will gain the capacity to interact with and control a diverse array of robotic platforms via multiple modalities, among which non-invasive Electroencephalography (EEG)-based interfaces remain the most widely utilized. Furthermore, IMARC Group forecasts that the social robotics market will experience exponential growth, reaching an estimated $36.6 billion by 2032, driven by a Compound Annual Growth Rate (CAGR) of 25.2% between 2024 and 2032. The deployment of billions of connected devices across these two overlapping domains will be fundamentally accelerated by structural advancements in cloud infrastructure, AI, and the Internet of Things (IoT). This technological convergence will ultimately facilitate the seamless integration of BCI hardware and robotic agents into domestic, clinical, and corporate environments.

The widespread proliferation of AI-driven conversational robots and non-invasive BCIs creates an urgent need for novel integration methodologies across sectors requiring innovative HRI. These sectors include education, customer service, loyalty programs, healthcare, social integration, rehabilitation, and smart home ecosystems. However, establishing seamless cognitive interactivity between humans and robotic agents presents significant technical and cross-disciplinary challenges. A primary obstacle resides in the biosignal pipeline: the preprocessing, feature extraction, classification, and subsequent translation of neural data into actionable robotic commands require tight collaborative orchestration among neurologists, biomedical engineers, and computer scientists. This interdisciplinary dependency is further complicated by a widespread shortage of specialized domain expertise and persistent difficulties in replicating experimental results. Consequently, accurately decoding human intent from raw, highly non-stationary Electroencephalography (EEG) signals remains a formidable barrier for computer scientists developing consumer-facing BCI software applications.Furthermore, software fragmentation presents a major architectural bottleneck, as the majority of existing BCI applications are proprietary and hardcoded for specific hardware devices or single-use deployment scenarios. While this lack of interoperability in BCI-robot integration has been partially mitigated through Internet of Things (IoT) communication protocols—where "brain-to-IoT-object" pipelines leverage specific frameworks like MQTT or OPC UA—these architectures require advanced, multi-language programming expertise. Such highly specialized technical skills are typically absent within target user domains like education, retail, or clinical care.To overcome these barriers, an innovative "brain-to-IoT-robot" communication methodology is required to seamlessly abstract robotic platforms into standardized IoT nodes. This methodology must introduce novel integration frameworks and algorithms that connect BCIs with social robots via ubiquitous, standard HTTP GET and POST requests, bypassing the need for complex, specialized industrial protocols. Such an approach will decouple hardware from software, broadening the interoperability of heterogeneous BCI devices with diverse social IoT robots while drastically lowering the programming threshold for developers. Ultimately, this architecture will enable the efficient offloading of raw EEG telemetry to cloud infrastructures for rapid neural data analytics, while concurrently allowing social robots to leverage cloud-based Natural Language Processing (NLP) services to dynamically translate decoded cognitive and emotional states into natural, contextual speech.

Aim and objectives of the dissertation

The main aim of this dissertation is to develop and validate a universal methodology for integrating heterogeneous Brain-Computer Interface (BCI) devices and social robots within the Internet of Things (IoT) ecosystem, with subsequent experimental validation in the field of neuromarketing.

To achieve the main goal of the dissertation, the following specific objectives must be fulfilled:

1) Analysis of scientific achievements from home and abroad in the subject area of the dissertation. Study of existing BCI devices, social robots and possible areas of their application.
2) Systematic analysis of existing software platforms for integrating EEG-based BCI and social robots in the Internet of Things. Research on methods for transforming social robots into IoT "things" depending on their hardware and software configurations. Research on statistical and machine learning methods for characterizing and classifying EEG signals in decision-making or choice.
3) Research and design of a novel methodology for integrating BCI and social robots into IoT for various object domains. Development of original methods and algorithms for integrating various devices for BCI and social robots using the Node-RED platform.

4) Validation of the proposed methodology with an openBCI device and a social robot Furhat, with application in the field of neuromarketing for studying the spontaneous emotional reactions of consumers to product advertising and their choices. Development of experimental and demonstration software.

Research methodology

Novel methods for processing raw Electroencephalography (EEG) signals have been developed, introducing a unique neuromarker based on the geometric similarity of the second derivatives of signal power calculated within sliding windows. This approach is combined with a spatio-temporal similarity analysis of these temporal profiles using Pearson correlation coefficients (r).The investigation revealed a distinct negatively correlated dynamic ($r < -0.6$) within the theta frequency band across the frontal and central cortical regions. These findings align robustly with established international literature linking frontal theta activity to affective (emotional) evaluation and cognitive decision-making processes.To ensure statistical rigor, the dynamic analysis results were aggregated using Cohen's (d) effect sizes accompanied by (95%) confidence intervals (CIs) to differentiate between "like" and "dislike" behavioral responses. The statistical validation demonstrated that theta frequencies at channels AF3, F3, C3, AF4, Pz, and P4 serve as the most informative features during spontaneous, purchase-related reactions and decisions. Additionally, statistically significant secondary effects were observed within the alpha band at F3, Pz, T8, and T7, as well as the beta band at Cz and Pz.The proposed methodology demonstrates that this novel neuromarker provides a computationally efficient framework for the real-time analysis of spontaneous cognitive reactions to marketing stimuli. Concurrently, the application of Cohen’s (d) with corresponding confidence intervals guarantees statistical robustness by validating the stability and reproducibility of the observed neurophysiological variances across different stimuli.

Scientific publications

The main results of the dissertation work have been published in 3 articles, issued in the period 2022-2026. They have been reported at two international conferences, 2 of which have been invited for publication in a journal. A list of publications is given at the end of the abstract of the dissertation.

Noted citations

There are 5 noted citations for the presented publications. A list of citations is presented at the end of the abstract..

Scope and strcture of the dissertation

The dissertation consists of an introduction, 4 chapters, a general conclusion, contributions, a list of references and three appendices. The dissertation is developed in a total volume of 177 pages, contains 2 tables and 35 figures, the numbers of which in the abstract coincide with those in the dissertation. The numbering of the points and subpoints also corresponds to that of the dissertation.

II. Contents of the dissertation

Chapter 1 A REVIEW OF BRAIN-MACHINE INTERFACE AND SOCIAL ROBOTS WITH APPLICATIONS IN VARIOUS FIELDS

1.2 Overview of Brain-Machine Interface

1.2.1 Study of literary sources and achievements around the world in the area

The main approaches, technologies and methodologies used in the development and implementation of BMI in various application areas are analyzed. The main challenges related to effective interaction between BMI and social robots have been studied and systematized.

1.2.2 Nature of EEG signals

EEG stands for "electroencephalography", which is an electrophysiological process for recording the electrical activity of the brain. The electrodes of an EEG device capture this electrical activity, which is transformed into different EEG frequencies using a fast Fourier transform (FFT). Brain waves are generally categorized into five main types of frequencies: gamma, beta, alpha, theta and delta. Frequency, which refers to the speed of electrical oscillations, is measured in cycles per second. The brain waves studied in this dissertation are: gamma (30-45Hz), beta (13-30Hz), alpha (8-12Hz) and theta (4-8Hz).

Fig. 1 Emotiv EPOC+ BMI device

1.2.3 Review and study of existing BMI devices

For the purposes of the dissertation, the two EEG-based MMI devices used are examined in detail: Emotiv EPOC+ and OpenBCI. EPOC+ is an EEG device (Fig. 1), with a sampling frequency of 256Hz, and data transmission via a wireless connection - Bluetooth. EPOC+ has 14 electrodes, which are located on the scalp in accordance with the 10-20 system for EEG, which allows recording of raw signals of brain activity, as well as converted into different types of brain frequencies, alpha, beta, theta and gamma. EPOC+ is compatible with Emotiv software (Emotiv PRO, Emotiv BCI, Emotiv Insight App). Among the main advantages of EPOC+ are its portability and ease of use, which makes it convenient for field research. The BCI device has good resolution and is affordable. However, EPOC+ requires additional maintenance of wet electrodes, which makes it inconvenient for users.

OpenBCI is an open source software platform for biosignal acquisition, designed to provide an affordable solution for research in the fields of neuroscience, bioelectronics and MCI. OpenBCI offers several models of BMI devices for measuring EEG activity, as well as muscle activity (EMG) and cardiac activity (ECG). The OpenBCI device provides a variety of configurations with different numbers of electrodes and sensors, allowing users to design the most suitable option for their research. For the purposes of the dissertation, the technical characteristics of the OpenBCI Ultracortex MMI device operating with Cyton and Daisy modules (Fig. 2), equipped with chips from Texas Instruments, are examined.

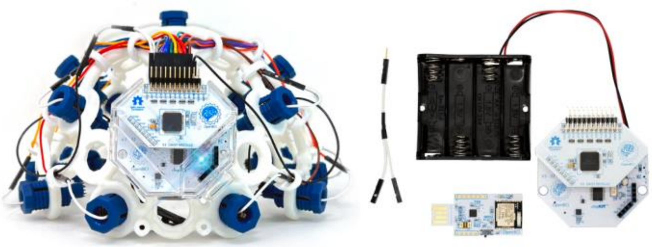

Fig.2 OpenBCI Ultracortex (with Cyton и Daisy modules)

Each module has 8 input channels for EEG electrodes, which provides sufficient coverage of brain activity. The Ultracortex EEG device supports up to 16 electrodes.

1.3 Overview of social robots

Social robots are increasingly being used in areas such as social assistance, financial services, and retail, as they have the ability to adapt their behavior to the needs of users. In social assistance, these robots help the elderly and people with disabilities by providing assistance with daily tasks and providing social interaction. In financial services, they automate customer interactions and improve service through intelligent systems. In retail, social robots improve the customer experience by providing real-time information and assistance. Social robots are increasingly integrated with IoT systems, allowing for better interaction and control in smart environments. These robots can act as central hubs for managing IoT devices, offering users a seamless experience in home or business automation through voice commands, touchscreens, or facial recognition. The social robots used in the research are Pepper and Furhat.

Pepper (Fig. 4) belongs to a family of humanoid robots developed by Softbank Robotics. It is 120 cm tall and weighs 28 kg. With its motors located in the neck, shoulders, elbows, wrists, fingers, waist and knees, the robot has 20 degrees of freedom. With its three omnidirectional wheels, the robot can move freely. Through its input and output devices, the robot interacts with a person. It has four microphones, two speakers, two 2D cameras and a 3D camera, all located in the head. It has a multilingual interface supporting 15 languages. Pepper has six lasers, two infrared sensors, two sonar, two magnetic encoders and an inertial unit, which are responsible for its independent movement. Pepper has a tablet that can be programmed in JavaScript and HTML, and it is possible to play various audio and video formats, as well as web pages.

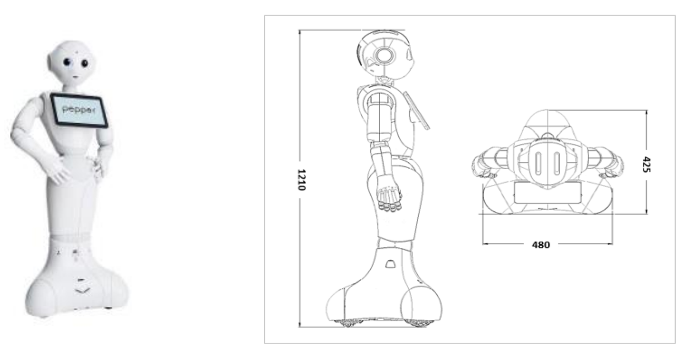

Fig.4 Pepper robot

The robot has preinstalled NAOQi operating system, which can be programmed with the following languages: Python, Javascript, C++, ROS. To access the robot system and control its behavior, Choreographe or Pepper SDK is used, which have pre-created control blocks.

The social robot Furhat (Fig. 6) was produced in 2011 by Furhat Robotics, and in 2018 the second hardware version was released on the market, as well as new versions of the software for its management – Furhat OS and SDK.

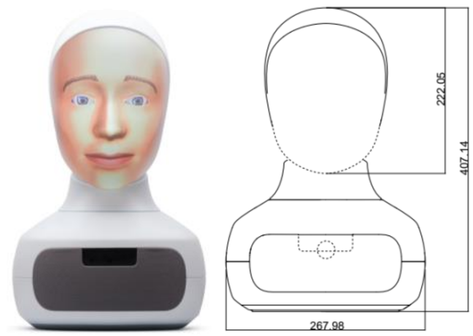

Fig.6 Furhat robot

Furhat measures 41x27cm. It has 2 microphones and two speakers. Additionally, a USB device with 4 more microphones can be used, thus the range reaches 5 meters. Furhat has a 3D printed head with a translucent screen on which a face is projected. The projector provides facial animation that can be customized for different genders, races and ages. The expressions are realistic, and their flexibility is determined by the possibility of changing the eyes, lips and facial movements during contact with the robot. A color camera is installed to register a person in its workspace and monitor its behavior. It has facial and voice recognition in different languages, recognition of facial expressions and gestures. Its built-in operating system FurhatOS and SDK allow complex behavior models to be developed using skills in the Kotlin programming language.

1.4. Overview analysis of the integration of BMI and social robots

1.4.1. EEG-based brain-robot interaction

By placing an MMI device with a set of electrodes, brain signals can be registered, classified and transmitted in the form of commands to control a robot. EEG-based brain-robot interactions are active and passive. An example of passive interaction is the detection of engagement in a person. Engagement indicates cognitive and emotional commitment to a given task. The goal of the method is to compare or correlate EEG signals with the intentions and emotions of the user. 4 processes have been defined in brain-robot interaction. The first of these is the collection of EEG data through the electrodes of the device. This is followed by filtering and processing of the collected signals. The next process is data classification, often using methods such as SVM (Support vector machine), RL (Reinforcement learning), CNN (Convolutional Neural Network), but descriptive and inferential statistical approaches are also applied. This is followed by the translation of the recognized intentions into direct commands to the robot or indirect communication - adapting the robot's behavior to the human state. The EEG data collected in this way can be used to identify errors in the robot's behavior, as well as to detect emotions, concentration, and mental fatigue in humans.

In this dissertation, the integration of MMI and social robots is applied in neuromarketing, as it offers innovative opportunities for more credible marketing strategies by assessing consumers' subconscious purchasing decisions.

1.4.2. Consumer neuromarketing

Neuromarketing uses the tools of neuroscience to determine why we prefer certain products over others. Neuroscience studies brain activity while we make choices..

When tracking brain function, neuroscientists typically use either electroencephalography (EEG) or functional magnetic resonance imaging (fMRI) technology. Different brain wave patterns are assessed to track the intensity of reactions such as anger, pleasure, disgust, and excitement. Activity in a particular brain region can predict future purchase of a product or experience. The prefrontal cortex (PFC), located in the frontal lobe of the cerebral cortex (FC), plays a key role in basic human decision-making processes. People can be attracted or repelled by a stimulus when they interact with it. Researchers are currently investigating brain activity signals that are associated with increased emotional involvement when people interact with marketing stimuli. According to EEG power spectral analysis, the left prefrontal cortex appears to be a significant component of a brain circuit that plays a key role in controlling or regulating behavior related to reward or pleasure seeking, while the right PFC appears to be a key component of a neural circuit that plays a key role in regulating behavior related to protection from adverse stimuli. Overall, research on existing neuromarketing approaches shows that there is no universal and validated framework to predict consumer purchase intention through EEG signals. Furthermore, EEG-based studies on consumers' affective attitudes towards different types of advertising stimuli are almost lacking.

Conclusions on chapter 1

The revolution of social robots is significantly changing the way they are used in assistive activities, such as banking services and marketing technologies and channels. By integrating a BMI with social robots, an improvement in the quality of services in various object areas can be achieved. Therefore, the dissertation proposes a concept for the use of the IoT, in which sensors, devices, calculations and memory can be easily integrated into a single platform that is independent of the type of devices or services.

CHAPTER 2 SYSTEMATIC RESEARCH OF SOFTWARE METHODS FOR DESIGNING AND INTEGRATION OF EEG-BASED BRAIN-MACHINES INTERFACE AND SOCIAL ROBOTS IN THE INTERNET OF THINGS

2.1. Software platforms for integrating BCI and social robots into IoT

This chapter provides an overview of the available software solutions used for the integration of MMIs and social robots into the IoT. Existing platforms, tools and technologies that enable the effective connection and interaction between MMIs, social robots and various IoT devices are presented, emphasizing their advantages, disadvantages and potential for future development in the context of various applications and scenarios. The focus is on the Node-RED platform used in the research, as well as the protocols used for the transformation of social robots into IoT "things".

Node-RED is a widely used platform for developing IoT applications because it uses visual programming and is flow-based programming by "connecting" pre-coded blocks. Editing and programming flows is done in a browser. Node-RED is a tool that is based on Node.js and provides an environment for developing applications in the Internet of Things (IoT). It is built on Chrome's JavaScript engine V8 and is a cross-platform environment for server-side execution of scalable applications using JavaScript. The basic building block in Node-RED is the node. Nodes are triggered when they receive messages – either from a previous node in the flow or from an external event. Once connected to a flow, nodes can wait for an external HTTP request, timer, or hardware change. Nodes process incoming messages and either forward them or generate new messages that are sent to subsequent nodes in the flow. Messages can be shared between nodes, even across different flows. Through the Emotiv-BCI nodes in Node-RED, the EPOC+ device interface can be used to collect and share neural data. Npm and Node.js play a key role in the Node-RED platform, providing the necessary infrastructure for development and package management. Node.js is an asynchronous, event-driven JavaScript runtime that enables the building of scalable and efficient network applications, such as Node-RED. Npm, in turn, is a package manager that makes it easy to install, publish, and manage software modules needed to extend the functionality of Node-RED. With npm, developers can easily add new nodes and libraries to Node-RED using the large collection of packages created for Node.js and shared in the community. This combination allows for flexible and dynamic creation of flows and applications in IoT and web environments.

2.2. Methods and algorithms for programming social robots in the context of their transformation into IoT "things"

2.2.1 Methods and algorithms for programming Pepper robot

To program the social robot Pepper and create specific applications, Choreographe, a platform for developing behaviors and functionalities, is used. It offers a visual interface that allows users to create and manage complex scenarios and interactions without programming skills. Choreographe uses graphical blocks and modules (Fig. 13) that can be connected and configured to implement the desired behavior of the robot.

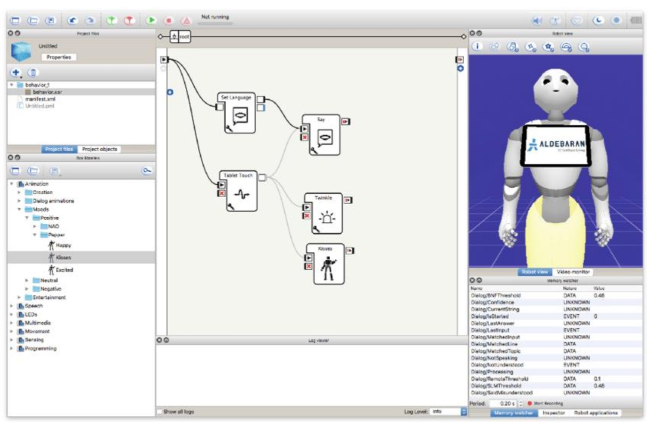

Fig.13 Programming Pepper in a specialized software platform Choreographe

In Choreographe, each block can be set up and configured to perform specific actions, such as controlling the robot's movements, activating voice or visual commands, and interacting with users. Blocks can be connected together to create logic for complex scenarios, such as managing dialogues, coordinating gestures, and reacting to specific events. Creating dialogues and scenarios allows you to define how Pepper will respond to different commands and questions. Choreographe offers a simulator to test the skill before implementing the project on the physical robot. The project can be launched and controlled directly by the robot, providing the necessary behavior in response to user reactions.

2.2.2. Мето Methods and algorithms for programming Furhat robot

Furhat is a social robot designed to provide intuitive and natural interaction with people. Furhat integrates the most advanced technologies for natural language recognition, facial gestures and emotions. The platform architecture includes two main components – skills and a hosted graphical user interface (Hosted GUI), through which both verbal and visual forms of interaction with the robot are implemented. Creating skills for Furhat requires the use of the Kotlin programming language, which provides tools for developing complex interactive dialog applications. The capabilities of skills include controlling the robot's voice, performing gestures, expressing various emotions, reacting to input events, and more. Furhat SDK (Fig. 14) provides a set of libraries and algorithms that facilitate this process, including ready-made scenarios. Furhat SDK also offers simulation and testing of a virtual robot. Creating a skill for Furhat is implemented using the Furhat SDK Launcher in the IntelliJ IDEA environment, with the project configured as a Gradle project with the necessary dependencies and versions of Kotlin and Java. An essential stage of the process is the development of the skill logic in the src directory, where the main files with unique names that enter the dialogue hierarchy and control the robot's behavior are created and modified. When working with a physical robot, it is necessary to create a configuration for connecting to it and starting the corresponding robot skill. After successful testing, the project is packaged in a .skill file using a Gradle command, which allows it to be launched using the SDK Launcher or via the command line. After installing the skill in the robot via its web interface, it can be launched manually or configured to run automatically when the device starts. Hosted GUI is a web-based application designed to provide a graphical interface for interacting with Furhat. It can be developed using web technologies such as HTML, CSS and JavaScript, and works based on sending commands and events to the robot, as well as receiving information about its current state, actions and dialogue reactions.

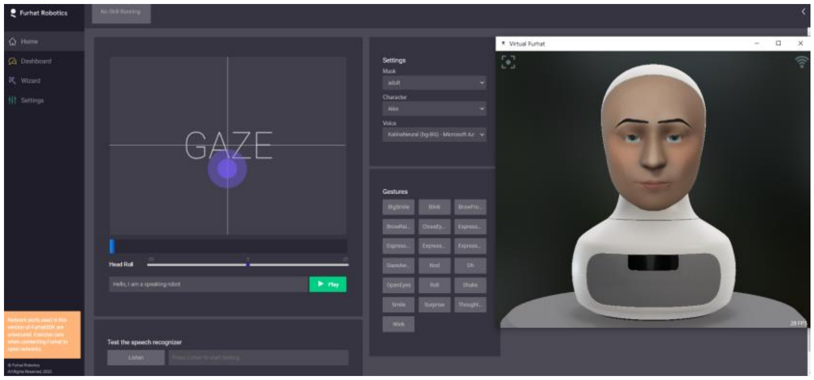

Fig.14 Furhat SDK

Hosted GUI not only improves the interaction between users and Furhat, but also provides additional functionalities that include data visualization, control of specific parameters, and collection of user feedback through touch communication..

2.3. Transformation methods for social robots into IoT “things”

There are various methods for converting a device into an IoT “thing”. The most commonly used method is through standard data exchange protocols (MQTT, OPC UA, Kafka, RabbitMQ, REST, XMPP, Google Cloud Messaging), using either a client-server or an event-driven publish-subscribe architecture. During the doctoral research, a more universal way to transform social robots into IoT “things” was also sought – by implementing the HTTP protocol, which all modern servers support, and the most commonly used methods POST and GET.

However, the most popular protocol for IoT use is MQTT (Message Queuing Telemetry Transport), which is implemented and tested in the dissertation. MQTT is a client-server protocol for exchanging messages using the publish-subscribe model. It is lightweight, open, and designed to be easy to implement. When implementing the publish-subscribe protocol, applications connect to a broker to publish messages or subscribe to topics to receive published messages. The central component of MQTT is the MQTT broker, which implements the MQTT specification.

Another application and test in the dissertation is the HTTP protocol, and novel methods and algorithms for IoT integration of MMI with social robots have been investigated through the widely used HTTP GET and POST requests, which are easily accessible and do not require specialized protocols. This will expand the connectivity of different MMI devices with different types of social IoT robots, while simultaneously facilitating programming. By using HTTP POST and GET requests, a device can send data to or receive data from a server or another device. POST and GET requests are used to exchange data between IoT devices and with other systems or services. Using Node-RED, flows can be created that manage this data exchange, making the device part of an IoT ecosystem. Node-RED supports this integration through the built-in node for http-endpoints. By using Node-RED to process HTTP requests, the device can participate in the wider IoT network, facilitating data exchange and integration with other IoT devices and services. Sending HTTP POST and GET requests to Node-RED can be considered part of turning the device into an IoT object.

2.4. Research on machine learning methods for characterizing and classifying EEG brain signals during decision-making

After the EEG signals have been registered, pre-processed to remove interference or noise caused by muscle movements, eye blinks, and heartbeat artifacts, they must be classified. At this stage, the Principal Component Analysis (PCA) and Independent Component Analysis (ICA) methods are widely used. To extract various characteristics of the pre-processed EEG signals, the most commonly used methods are the Fourier Transform and its derivatives Short Time Fourier Transform and Fast Fourier Transform. The disadvantages of these methods are that they do not have characteristics regarding the time domain of the received signals. In the 1980s, a new signal processing method was invented - Wavelet Transform, and it is widely used in classifying the received EEG signals to this day.

The most commonly used machine learning methods for feature extraction for the purpose of classifying EEG signals are Support Vector Machine (SVM), Artificial Neural Networks (ANN), Convolutional Neural Networks (CNN), k-Nearest Neighbors (k-NN), Linear Discriminant Analysis (LDA), Logistic Regression and others.

2.5. Research on statistical methods for characterizing and classifying EEG signals

When studying EEG characteristics, the average power in a given frequency band is often used in various statistical tests for comparison between conditions or groups. The most common combination is ANOVA and t-tests, which allows inferentially assessing differences in EEG data both between multiple conditions and between specific pairs of conditions, providing a reliable statistical analysis of brain activity.

2.5.1. Classical methods for analysis and comparison of EEG characteristics

The most commonly used one-way ANOVA analysis is used when there are more than two experimental conditions (for example, “rest”, “cognitive task” and “visual stimulus”). This analysis checks whether the mean values of the selected EEG characteristic differ statistically significantly between the conditions. If the result is significant, this means that at least one of the conditions differs from the others in terms of the measured characteristic and the Null Hypothesis is confirmed or rejected.

Another commonly used test is the independent samples t-test. It is used when only two conditions are being compared (e.g., "stimulus" versus "baseline"). The test checks whether the mean values of the EEG characteristic in the two conditions are significantly different.

Descriptive Statistics aims to summarize and describe the main characteristics of a given data set, without testing hypotheses or making predictions, but only organizes and presents information systematically through characteristics such as mean, median, standard deviation and frequency distributions. A major drawback is that statistical analysis does not show how signals from different electrodes and brain regions vary over time, i.e. signal dynamics.

2.5.2. Method for descriptive and inferential statistical data analysis

Descriptive and inferential statistical methods were used to analyze the EEG data. These approaches include Pearson correlation analysis and Cohen's effect coefficient, the application of which is discussed in more detail in section 3.6.3.

2.6. An innovative model for transmitting, analyzing and processing EEG signals and converting them into commands for interaction with social robots in IoT

As a result of the systematic study of software methods for designing and integrating EEG-based MMIs and social robots in IoT conducted in this chapter of the dissertation, a conceptual model (Fig. 16) is proposed for transmitting, analyzing and processing EEG signals, and their conversion into commands for social robots in IoT. The model presents interaction with a social robot through MMI based on integration in the Node-RED platform, which provides easy connectivity with IoT devices and services. The platform's communication with the social robot can be performed via HTTP protocol and GET/POST requests or MQTT protocol, which allows reliable transmission of data and commands between individual components. The EEG-based BCI device can be connected to Node-RED via Wi-Fi or Bluetooth, while the social robot can be connected only via Wi-Fi. The diagram shows the entire data flow starting from the transmission of EEG signals to the BCI device, which are then transmitted to Node-RED. The Node-RED IoT platform processes and routes information, then sends the corresponding commands to the social robot and/or IoT devices and services. These commands can be transmitted via existing Node-RED nodes such as HTTP GET/POST, MQTT, WebSocket, BLE, and others. The model envisages that Node-RED will communicate with the social robot via an API, which can be embedded in the robot itself or via a remote service.

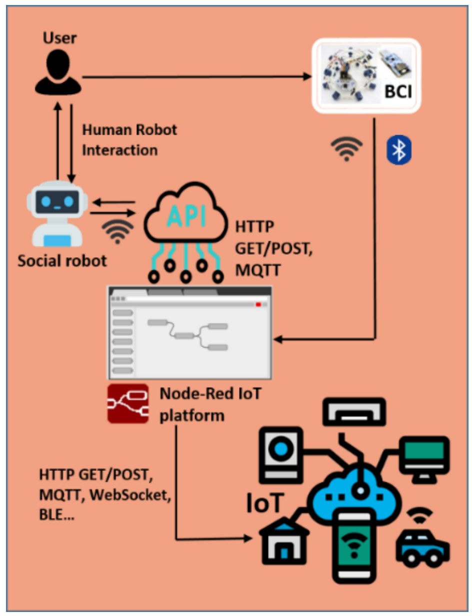

Fig.16 An innovative model for interacting with social robots via EEG signals in IoT

Conclusions on chapter 2

Advantages of BCI in IoT - integration of various EEG devices with the ability to transmit EEG data, characteristics and metrics over the Internet without programming skills, MMI and social robots in IoT, easily connect them to MMI "things" and thus easily configure the device, data type and desired electrodes, based on which the corresponding application programming classes (API) with the necessary arguments can be called in IoT.

CHAPTER 3 DEVELOPMENT OF ORIGINAL METHODS AND ALGORITHMS FOR INTEGRATION OF BRAIN-MACHINE INTERFACE AND SOCIAL ROBOTS

3.1. Novel methods for EEG-based brain-robot interaction in IoT

The solutions for EEG-based Brain-Robot communications in IoT reviewed in the scientific literature are mostly tied to a specific platform, device or application scenario. Therefore, in this dissertation, a novel more universal approach for communications between different MMI technologies and social robots in IoT is proposed using the Node-RED platform. The proposed method for EEG-based brain-robot interaction allows the MMI device and the robotic system to be transformed into IoT “things” through a cross-platform server-side execution environment integrated into a browser environment. In this way, individual components can exchange, share and process data with minimal human intervention, using a publish–subscribe communication model. This approach provides a high degree of flexibility, modularity and the ability to integrate heterogeneous devices and services into a single communication architecture. An additional advantage of the proposed solution is the ability to implement various cloud integrations through the FRED platform, which provides a cloud environment for hosting and managing Node-RED applications.

The proposed method allows the integration of the Emotiv EPOC+ MMI device and the humanoid robot Pepper in Node-RED. Nodes for the EPOC+ device have been developed in the Node-RED palette, but none exist for Pepper. However, since there are nodes in Node-RED for executing external processes such as pythonshell, exec or ros, system commands, Python scripts or ROS processes can be executed to communicate with Pepper. The Emotiv-BCI Node-RED Toolbox is a customized library of input nodes for Node-RED that allows the interaction of EMOTIV technology with Node-RED.

The proposed method for building a brain-robot interface in IoT based on EEG allows the integration of the OpenBCI MMI device and the Furhat social robot in Node-RED via the OpenBCI Toolkit for Node-RED. This toolkit uses the BrainFlow library in the Node-RED platform and can be applied to more than 20 EEG devices. It is built from three nodes - the "openBCI-streaming" node launches the main process to the OpenBCI board in Node-RED. The "openBCI-data" node executes an algorithm that either accesses raw data from the EEG device, processes it through predefined filters, or calculates the power of six frequency bands of the EEG signal in real time. The last node "openBCI-EEGmetrics" registers the focus levels of the subject connected to the EEG device.

3.2. Transforming Pepper into an IoT device and integrating it with an EMOTIV EPOC+ device for BMI

3.2.1 Through MQTT broker

The transformation of the Pepper robot into an IoT device (Fig.17) has been studied and designed, implementing the MQTT protocol on the robot side to connect to an MQTT broker that listens to the published data in topics. The robot is installed with the qi Framework for programming, which starts and establishes a communication session (qi.Session) with the robot control operating system - NAOqi. The open source Eclipse Mosquitto broker is used, running locally on the computer where the qi Framework is installed..

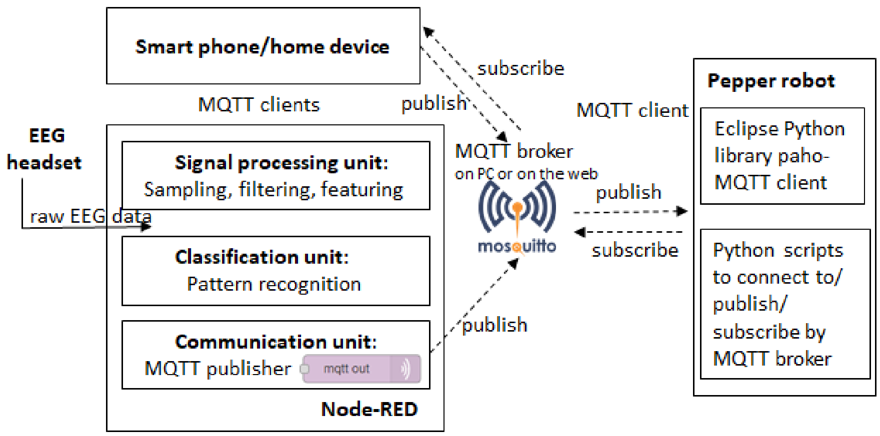

Fig. 17 Transformation of Pepper into an IoT device based on an MQTT broker

An example scenario was tested to validate the proposed approach - Pepper wakes up or rests depending on the published message with the topic "goToPosture". The "wake-up" message is parsed in a Python script by NAOqi ServiceManager, which sends a command to the robot to wake up via "session.service("ALMotion").wakeUp()". Similarly, if the published message is "rest", Pepper goes into rest mode via "session.service("ALMotion").rest()". Messages can also be published from an MMI stream in Node-RED and sent to the broker via an mqtt-out Node-RED node. For example, depending on the current emotional state of the user, as assessed by the MMI, messages to a predefined topic "valence_state" can improve the ALMood module, which is responsible for recognizing the emotion of the person in front of the robot.

3.2.2 Through mqtt nodes in Node-RED

A second approach to transform Pepper into an IoT device has been researched and designed, which also uses the Eclipse Mosquitto broker locally or on the Internet, but the connection to the broker and the exchange of messages are carried out through mqtt-in and mqtt-out nodes in the Node-RED platform (Fig. 18).

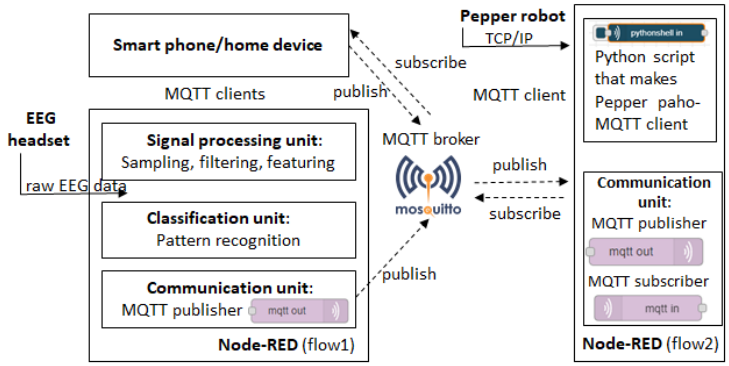

Fig. 18 Transformation of Pepper into an IoT device based on mqtt nodes in Node-RED

Pepper as an MQTT client connected to the broker, running NAOqi APIs from Node-RED instead of an external IDE. Pepper uses mqtt-in and mqtt-out nodes to publish-write to topics in Node-RED. IoT control of robot posture from MMI and robot control flows has been successfully validated by publishing-subscribing to the topic “goToPosture”. After publishing a “wake up” message from the mqtt-out node to the Mosquitto broker, the message is received as a “payload” on the mqtt-in node via the robot’s Python paho-MQTT client. Based on the received message and topic, parameters for the Python script are defined and sent to the pythonshell node to call NAOqi APIs.

3.2.3 Through a continuous process in the Python programming language

The third researched and designed approach to transform Pepper into an IoT device does not use an MQTT broker or MQTT nodes. It uses only Node-RED, which follows an event-based architecture implemented through a publish-write communication model and allows devices to interact asynchronously (Fig.19).

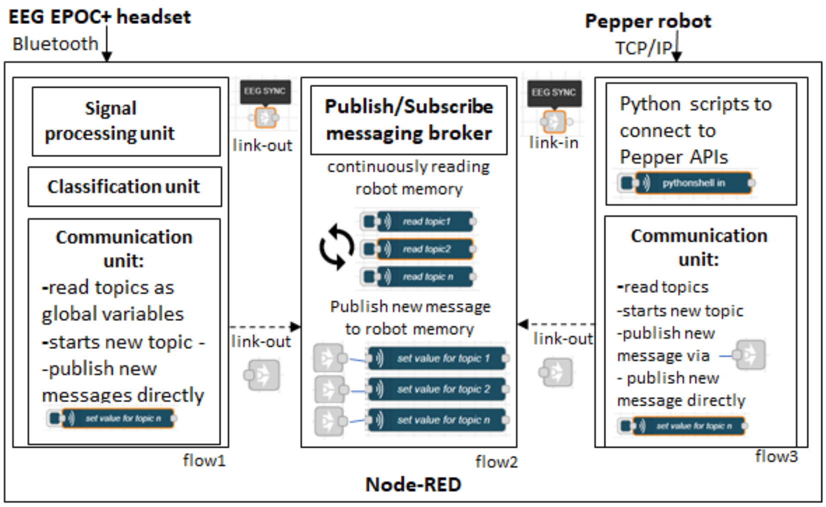

Fig. 19 Transformation of Pepper into an IoT device based on a continuous Python process for reading the robot's centralized memory from a stream in Node-RED

This approach uses Pepper's centralized memory not only for its current motor and sensor states, but also for storing and retrieving data using the ALMemory module methods in key-value format. Thus, the robot's memory is used as a data broker and is read/written to. ALMemory APIs are called via a continuous Python process in a Node-RED stream to provide the current value for the keys for which there are registered subscribers.

3.3 Methods and algorithms for integrating the Pepper robot into IoT

3.3.1 Developing a communication architecture in Node-RED for the Pepper robot

To perform the tasks set in the dissertation, a communication flow in Node-RED was designed to establish a connection between the Pepper robot and the message broker, record and process EEG data, and call the NAOqi API. The designed flow is presented in Fig. 20. It contains communication nodes, nodes with message processing functions, change nodes, JSON nodes, input/output flow nodes, and pythonshell nodes used to interact with Python processes. The presented brain-robot interface was developed in the context of neuromarketing. The first pythonshell in the flow (in the upper left corner of Fig. 20) expects to detect a person in the robot's workspace. Pepper then moves and offers interaction options on the touchscreen tablet (the second pythonshell in Fig. 20), where web content related to virtual marketing campaigns is visualized. The third pythonshell responds according to the ALTabletService::onTouchDown method, and depending on the coordinates of the selected virtual button, a mapping function converts the pixel coordinates into metric coordinates in the pre-modeled market environment, which determines the target position of Pepper (the fourth pythonshell). The button coordinates (screen image) are in pixels and a matching function is used to convert them into metric coordinates on the map. The fifth pythonshell loads the map according to the given argument and locates Pepper using ALNavigation::navigateToInMap([x, y, theta]). After reaching the given position, the robot uses the link-in nodes to obtain EEG data, according to the goals of the marketing campaign, and records them for subsequent analysis. The last pythonshell returns Pepper to its starting position.

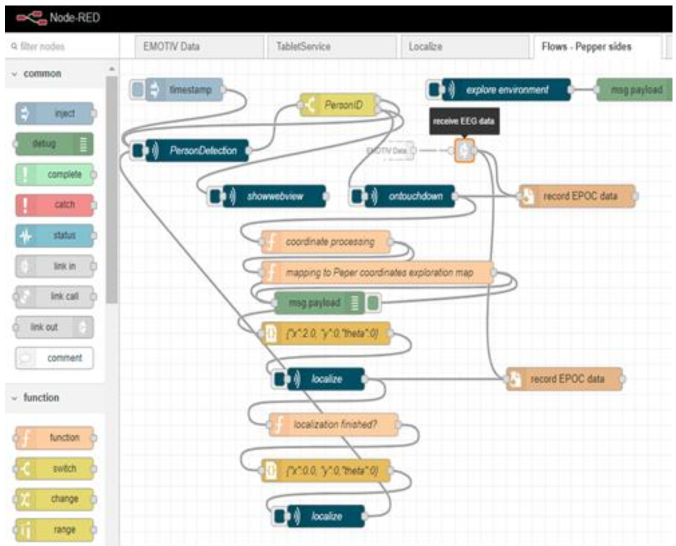

Fig. 20 Communication flow for obtaining EEG data and interface with the Pepper robot API in Node-RED

3.3.2 Algorithms for communication of EPOC+ with Pepper via Node-RED

A program flow for using the EPOC+ BCI device in Node-RED was designed and developed (Fig. 21). It implements the Emotiv library for Node-RED, which provides nodes for extracting the power of the theta and beta frequency bands for electrodes F3, F4, FC5, FC6, T7, P7, P8, O1 and O2.

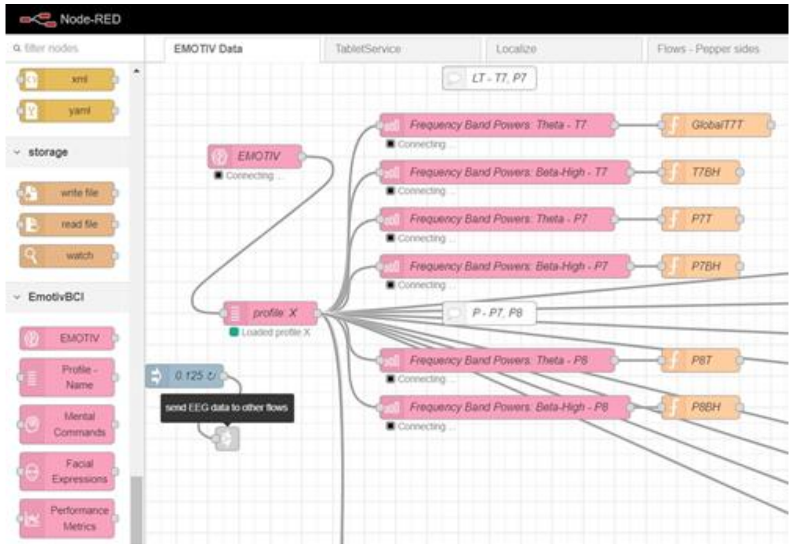

Fig.21 Flow for recording and transmitting EEG data in Node-RED

The proposed integration between BCI and Furhat is based on the exchange of data between nodes belonging to different flows in Node-RED. The data can be exchanged via global variables. An alternative method is to use link-out and link-in nodes. Global variables are used to send EEG data to Pepper and link-out and link-in nodes are used to synchronize the time points of the sent and received data – the link-out node in the BCI flow (Fig. 21) and the link-in node in the robot flow (Fig. 20). The publication and receipt of messages is performed via link-in and link-out nodes in the broker flow flow2 in Fig. 19. Via the link-out node, EPOC+ and Pepper send a value to a node from their flows (flow2 and flow3 in Fig. 19). Via the link-in nodes in the broker flow, the value is written to the robot memory via Python scripts. However, direct publication of messages without using a broker is also possible. An option has been developed for EPOC+ or Pepper to send a value for a given node from their streams directly via a Python script that calls the ALMemory API..

The integration between the MMI and the robot is designed and developed using a flow acting as a broker for the publish-subscribe method (flow2 in Fig. 19). It reads topics and messages through continuously running Python processes in Node-RED, which call the getData("topic_n") method of the ALMemory module to read topics of interest. The received topic messages are stored as global variables in the "key:value" format to be used by other flows in Node-RED. Publishing is done either by the broker or directly by a flow by calling the insertData("topic_n", "value_n") method of the ALMemory module. The advantage of the proposed solution is the simplification of the devices that need to be connected. Using the robot's internal memory to share and collect topic data allows publishing and subscribing to be done by other Node-RED modules or by external IDEs. Thus, synchronization can be easily maintained. The proposed approach is general enough and can be applied to other MMI devices or robots that do not have nodes in the Node-RED palette. These devices should be open source and programmable with Python or ROS..

3.4. Transforming Furhat into an IoT device

Designed and developed an original method for transforming Furhat into an IoT device, shown in Fig. 22. The transformation of Furhat into an IoT device is implemented by building a communication channel between the Kotlin skill and the Node-RED platform through the "http-in" node, functioning as an HTTP server that waits for incoming HTTP requests to a specified URL with GET/POST methods, but the specificity of the communication is the presence of a graphical user interface hosted by the Kotlin skill. When Furhat sends requests to the Node-RED server, they are blocked or delayed during the processing of events by the hosted React GUI application, which is solved by switching from synchronous to asynchronous HTTP requests, described in detail below.

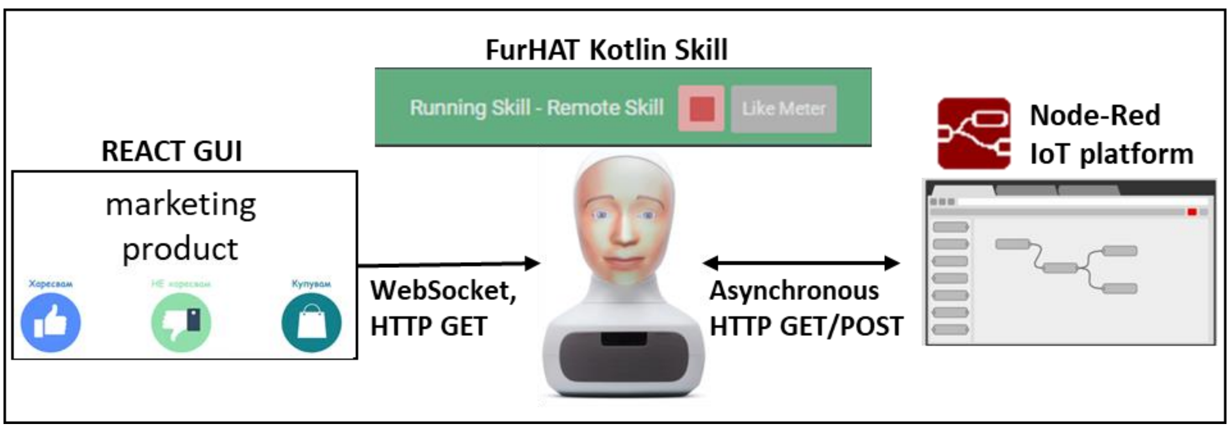

Fig.22 Transforming Furhat into an IoT device

For the purpose of developing a graphical user interface to visualize a marketing survey to the user in Chapter 4, a graphical user interface (Hosted GUI) and a FurHAT Kotlin Skill, created using a domain-specific-language (DSL) in the Kotlin programming language (FurHAT Kotlin Skill), were designed to control the dialog flow and send the user's preferences to Node-RED for synchronization with the EEG signals recorded for the current marketing stimulus.

The Furhat SDK allows adding graphical interfaces to Kotlin skills through a process for creating and hosting a web GUI directly from the skill. The Hosted GUI is built using React technology - a JavaScript library designed for building user interfaces that divides them into small, reusable components, such as buttons, text, and images. The survey contains five everyday products, and the user response options are three - like, dislike, and buy. JSX (a syntax extension of JavaScript) is used, and React is efficient through its virtual DOM, which updates only the changed parts of the interface. For the transformation in Fig.22, “HostedGUI” was used via the WebSocket API. This application programming interface allows the creation of a two-way interactive communication session between the user’s browser and a server, sending and receiving messages without the need for constant polling of the server for a response. The furhat-gui library opens a WebSocket connection to provide two-way real-time communication between the GUI and the Furhat skill. This is important when receiving events from the skill, as the WebSocket protocol is designed to provide low latency and two-way communication. The furhat-gui library uses an HTTP GET request for initialization and retrieval of data required for initial setup and configuration. The furhat-gui library provides access to the “furhat” object for the robot, through which events are sent to the Furhat skill, as well as the ability to subscribe to events from it. The dialogue flow in FurhatOS is based on a state diagram with advanced functionalities such as inheritance, global variables, and dynamic states, which allows for the implementation of complex interactions. The system is always in a specific state and makes transitions between individual states. In the marketing application developed in Chapter 4, the state defines the stages of decision-making, with each state controlling both Furhat’s behavior and the visual stimuli provided via the Hosted GUI. The state defines triggers that contain actions to be performed, including transitions between states, synchronized with the participant’s EEG recordings. The built interactive interaction used the “onEntry” and “onEvent” triggers to capture events sent by the Hosted GUI and mark time segments for EEG analysis. To overcome the identified conflict, where the Kotlin skill sends synchronous (blocking) HTTP requests to Node-RED, which hold up other processes and are blocked or slowed down during event processing by the hosted React GUI, asynchronous HTTP requests were used from the Kotlin skill via `CoroutineScope(Dispatchers.IO).launch { }`, allowing for the launch of parallel subroutines. For the experiment in Chapter 4, this allowed for simultaneous control of Furhat’s dialog behavior, visual stimuli, and processing of incoming EEG signals.

3.5. Methods and algorithms for integrating the Furhat robot into IoT

3.5.1. Development of a communication architecture in Node-RED for the Furhat robot

Once Furhat is transformed into an IoT device, it can be integrated into the Node-RED IoT platform through the designed Node-RED communication flow (Fig. 23), which registers and processes the requests sent by the Kotlin skill..

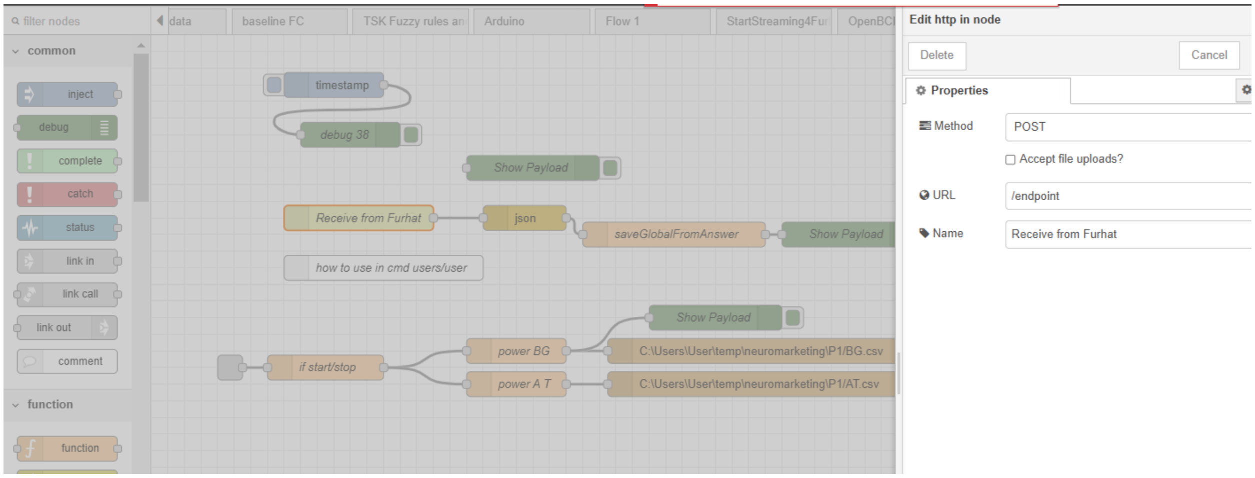

Fig.23 Communication flow for obtaining EEG data and interface with the Furhat robot in Node-RED

A key element in this communication flow is the "http-in" node in Node-RED, through the "http-in" node, functioning as an HTTP server that waits for incoming HTTP requests to a specified URL with GET/POST methods, and the content of the request is available via msg.payload. To connect to Furhat, a "POST" method and a "/endpoint" URL are required. When a request is received at this endpoint, it activates the flow, which allows the request to be processed and a response to be generated by other nodes in the flow. The response can be in the form of an HTML page, JSON, a text string, and other formats. In the built flow, the node's response is in the form of a JSON text string, and for its subsequent use, the request is converted into a JSON object by a JSON node. Since the "http-in" node does not send a response to the request, to complete the processing, the flow must use the "http-response" node, which generates and sends the response.

3.5.2. Algorithms for OpenBCI communication with Furhat via Node-RED

The integration of the transformed Furhat into an IoT device with an OpenBCI MMI device in Node-RED is shown in Fig. 24. This communication flow records, processes, and transmits EEG data in real time..

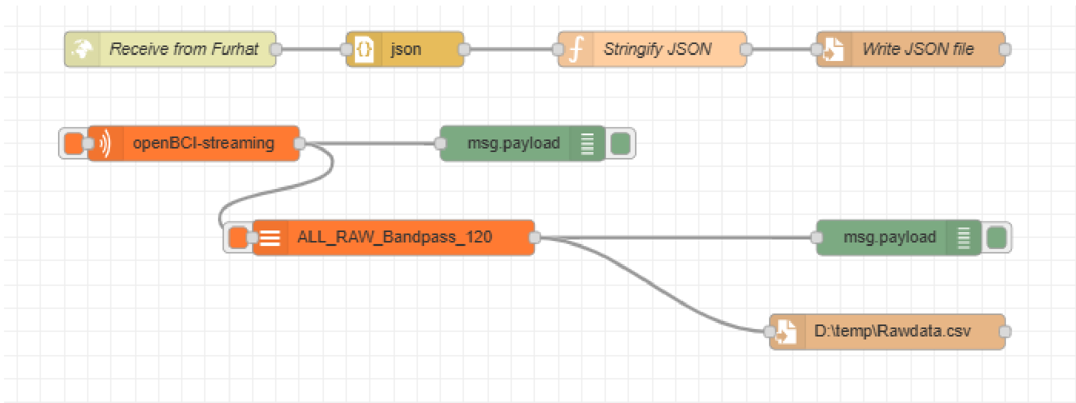

Фиг.24 Flow for recording and transmitting EEG data from an OpenBCI device to Node-RED

To achieve synchronization of the events registered by Furhat with the corresponding EEG data, i.e. to be uniquely identifiable from the beginning of the Furhat stimulus to its end in the EEG data array, an asynchronous process has been developed, through which the events from Furhat are recorded together with a timestamp of the event in a local json file, and the Node-RED node reads the information from this file and structures it by time in chronological order to the registered EEG data. This novel approach allows for asynchronous exchange of information between the robotic platform and the OpenBCI device, while ensuring the preservation of all events for subsequent processing. The process of registering data from the two end devices (Furhat and OpenBCI) and their synchronization begins with the first node ‚http-in' („Receive from Furhat" from Fig. 24) of the flow. It receives events generated by Furhat via HTTP protocol and transmits them to Node-RED nodes for appropriate formatting of the json object as a string, after which they are recorded by the next node in a local JSON file. After starting the EEG board via the "openBCI-streaming" node, the openBCI-data node ("ALL_RAW_Bandpass_120)" (Fig. 24) is activated, which provides access to the EEG data. A Python script, which is a child process of the openBCI-data node and is responsible for recording the EEG signals, periodically reads the contents of the JSON file, extracts each individual event to which it adds a time stamp in local Bulgarian time. In addition to the time of occurrence, each event is stored with additional information, such as "write" and "answer" markers, which serves for subsequent analysis of the participant's choice depending on the stimulus. After the events are read, they are associated with the time stamps of the EEG signals, thus each recording from the EEG device is associated with the specific event, which carries out the correlation between the participant's spontaneous reactions and the dynamics of their brain activity. Raw EEG data is acquired and preprocessed using the BrainFlow library, which provides an interface to the hardware, including configuration of channels, sampling rate, and timestamp synchronization. An additional node in Node-RED records the data to a file for subsequent offline correlation analysis of EEG activity.

3.6 Novel methods and algorithms for preprocessing raw EEG signals, feature extraction and classification under dynamic nonlinearity

EEG signals are characterized by high nonlinearity and temporal non-stationarity, which poses significant challenges for feature extraction and classification methods. Classical machine learning methods (SVM and kNN) and traditional statistical methods (ANOVA) are not accurate in analyzing neural data, as they rely on static features and assume mostly linear relationships, i.e. they cannot capture the fast dynamics and complex interactions between brain neurons from different brain regions. Methods such as Fourier transform and sliding window wavelet analysis provide detailed spectral and phase analysis, but are computationally intensive, making them inapplicable for real-time EEG analysis. Therefore, this chapter presents an original, lighter computational alternative to Fourier and wavelet analysis, suitable for real-time robotic systems, where the trade-off between computational efficiency and temporal resolution is a challenge.

3.6.1. A novel neuromarker based on spatiotemporal similarity analysis of power derivatives of EEG signals

The proposed new neuromarker is based on Pearson correlation between the second time derivatives of EEG power in sliding windows for different channels in the early response interval (0.5–2 sec). The size of the sliding windows was chosen based on a trade-off between temporal and frequency resolution. For theta (4–8 Hz) and alpha (8–12 Hz) frequencies, 0.5 second windows containing 62 counts (samples) were used. For beta (16–26 Hz) and gamma (25–40 Hz) frequencies, shorter windows of 0.25 seconds containing 31 counts (samples) were used. Spectral power was calculated separately for each frequency band and channel using segmented stimulus-specific subsets corresponding to the conditions “Like”, “Dislike” and “Buy”. The power spectral density was estimated using Welch’s method. To capture the dynamics of the signals over time, first- and second-order derivatives of the band power are calculated in overlapping windows. The first-order derivative determines the dynamics of the change in spectral power over time after stimulus presentation, while the second-order derivative reflects the acceleration of power changes, capturing sudden dynamics and non-stationary neural responses to stimuli. While the average power values and first-order derivatives may show similar patterns across stimuli, the second-order derivatives reveal obvious differences in the dynamic patterns across stimuli..

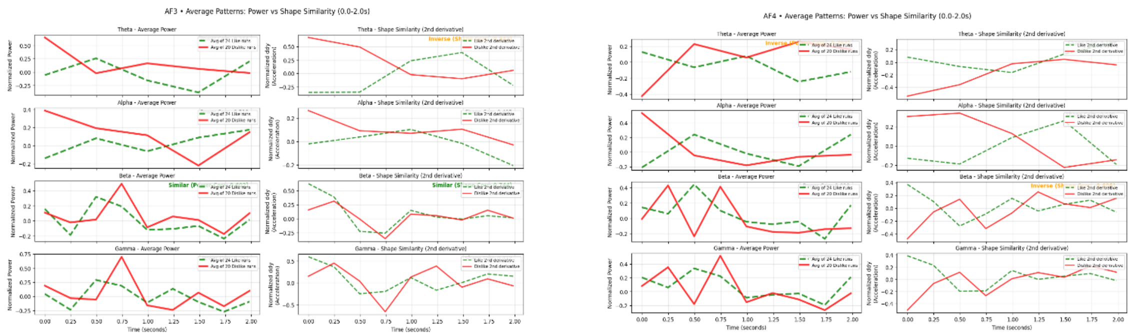

Fig.25 The average power versus second-order derivatives showing obvious differences in dynamic patterns between stimuli

3.6.2 Method for analyzing dynamic similarity of spatiotemporal results

The method assesses differences between stimuli by comparing the shape of temporal response patterns reflecting the spatiotemporal dynamics of spectral power *(P)* of the EEG signals.

To capture neural dynamics well, the analyses are based on time derivatives of spectral power per band and channel ($y'' = d^2P/dt^2$), thus emphasizing rapid amplitude changes and transient temporal variations, so as to reveal neural structures invisible in raw EEG data. Feature analysis focuses on the first 0.5-2 sec. after stimulus onset, corresponding to early decision making.

DTW revealed that the temporal shapes of the “Like” and “Dislike” conditions were very similar across most scalp regions, with similarity values close to 1 in the 0.5–2 s time window. Good discrimination was obtained using shape similarity based on Pearson correlation and cosine similarity calculated on the second-order derivatives of spectral power, with results showing largely identical patterns in both measurements (Fig 26). Pearson correlation was therefore used due to its lower computational complexity.

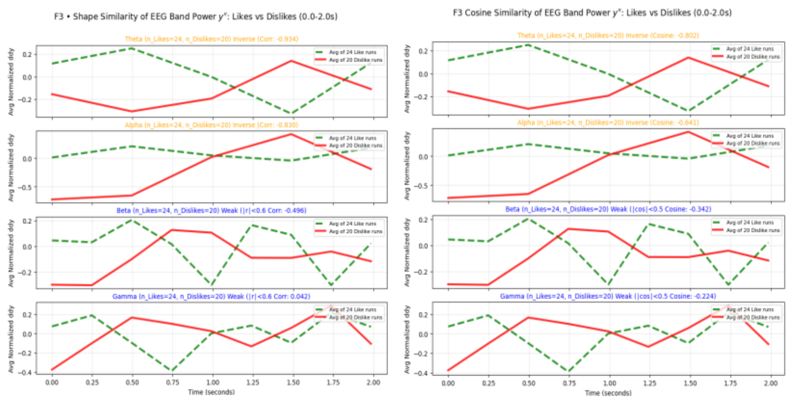

Fig.26 Shape similarity and cosine similarity based on Pearson correlation for channel F3

3.6.3 Methods for descriptive and inferential statistical data analysis

Formula (1) describes the proposed neuromarker. The Pearson correlation r_k within a window k of the second derivatives of EEG power in frequency bands and channels, calculated in sliding windows over the spontaneous response interval, quantifies the differences in spatiotemporal power dynamics between stimuli through the similarity of their temporal distortion. If $y_1''(t)$ and $y_2''(t)$ denote the second derivatives of spectral power for each band for two stimuli, w denotes the window length (in seconds), and k denotes the starting index of the sliding window.

$$r_k = \frac{\sum_{t=k}^{k+w}\left(y_1''(t)-\overline{y_1''}_k\right)\left(y_2''(t)-\overline{y_2''}_k\right)}{\sqrt{\sum_{t=k}^{k+w}\left(y_1''(t)-\overline{y_1''}_k\right)^2}\sqrt{\sum_{t=k}^{k+w}\left(y_2''(t)-\overline{y_2''}_k\right)^2}}, \qquad (1)$$

where

$$\overline{y_1''}_k = \frac{1}{w}\sum_{t=k}^{k+w} y_1''(t), \overline{y_2''}_k = \frac{1}{w}\sum_{t=k}^{k+w} y_2''(t) \qquad (2)$$

are the second-order averages for a window k.

Cohen's d (3) is calculated from the mean difference between conditions using pooled estimates of variance across trials. Confidence intervals are derived from the standard error of the effect size to assess statistical reliability. According to formula (5), the confidence interval is 95% across ranges and channels..

$$d = \frac{\mu_1-\mu_2}{s_p}, \qquad (3)$$

where

μ_1 – average value of features extracted from stimulus 1 (for example, the average value of $y_1''(t)$ in window k),

μ_2 – average value of the same characteristic, but for a stimulus 2,

s_1^2, s_2^2 – relevant deviations of the samples,

n_1, n_2 – number of attempts for each condition,

s_p – pooled standard deviation.

$$s_p = \sqrt{\frac{(n_1 - 1)s_1^2 + (n_2 - 1)s_2^2}{n_1 + n_2 - 2}}$$

Formula (4) defines the standard error in Cohen's d coefficient.

$$SE_d = \sqrt{\frac{n_1+n_2}{n_1 n_2} + \frac{d^2}{2(n_1+n_2)}} \qquad (4)$$

Formula (5) determines a 95% confidence interval.

$$CI_{95\%} = d \pm 1.96 \cdot SE_d \qquad (5)$$

The comparison of the second derivatives of the band power between two stimuli (S1 and S2) captures differences in power acceleration over time. Stimuli are considered distinguishable when the spatiotemporal curves are inversely shaped, i.e. their temporal dynamics are weakly or negatively correlated - a low Pearson coefficient indicates uncorrelated dynamics, while a negative d coefficient reflects an inverse temporal structure, highlighting a stronger distinction in neural processes. A threshold of $r \geq -0.6$ was chosen based on conventional correlation guidelines, where values ≥ 0.6 are usually interpreted as large effect sizes. Given the typical non-constant nature of EEG signals, a cosine similarity threshold of > 0.5 (corresponding to an angle $< 60°$) was chosen, which indicates significant directional alignment between the signals and is usually interpreted as reflecting significant similarity in the patterns.

Conclusions on chapter 3

This chapter presents a novel approach to integrate EEG-based MMI with a social robot for communication in an IoT environment. Node-RED is the chosen IoT tool through which the Emotiv EPOC+ device and the humanoid robot Pepper communicate. There is a library of input nodes in Node-RED for the EPOC+ device, through which it connects services and devices in the IoT, but such nodes are not available for Pepper. Therefore, three novel approaches to transform the robot into an IoT device are designed and tested. The devices share and collect data based on the publish–subscribe model implemented in Node-RED, and original flows for controlling the robot via MMI in an IoT environment are designed. In a similar way, a module for integrating OpenBCI and the Furhat robot in Node-RED was designed and developed, but the advantage here is that a universal HTTP communication protocol is used instead of the specialized MQTT protocol. A novel method, a combination of descriptive and inferential statistical data analysis, was also developed, which experimentally demonstrated significant discrimination of inverse spatiotemporal curves with inverse shape in the power of EEG signals. Pearson's correlation r_k was used to assess the linear dependence within a window k between the second derivatives of the power of EEG signals in different frequency bands and channels. The analysis was performed by applying sliding time windows within the studied interval, which allows tracking the dynamic changes in the dependences between the analyzed parameters. Cohen's coefficient d was calculated based on the average difference between the experimental conditions, using pooled estimates of the variance between individual trials. To assess the statistical reliability of the obtained effect size, confidence intervals were determined, calculated using the standard error of the effect size. This allows for a more precise interpretation of the significance and stability of the observed differences between the experimental conditions.

CHAPTER 4 EXPERIMENTAL TESTING AND VERIFICATION OF A METHODOLOGY FOR PREDICTING USER CHOICE BASED ON INTEGRATION OF EEG-BASED BRAIN-MACHINE INTERFACE AND SOCIAL ROBOT FURHAT FOR INTELLIGENT NEUROMARKETING

This chapter explores the development and experimental testing of the proposed in Chapter 3 Methodology based on the integration of EEG brain-computer interface and social robot Furhat. The main goal is to demonstrate how intelligent neuromarketing can use real-time data to predict and satisfy consumer preferences. The experimental studies cover the technical aspects of configuring the EEG device and processing the EEG data, as well as the synchronization between the information obtained from the EEG channels and the evaluation of products from advertising campaigns. Based on the proposed methodology in Chapter 3, software for neuro-analysis of consumer purchasing reactions to product advertising has been developed and experimentally tested. Based on the data obtained from the EEG-based OpenBCI MMI integrated with the Furhat robot, the results of 9 users have been summarized and the most significant electrodes and frequency bands for establishing human preferences and emotional evaluation (“like”/“dislike”/“buy”).

4.1 Experimental procedure for the scientific study

In order to fulfill the task of verifying the experimental software, a novel research procedure for ethical experimental research has been developed, approved by the Research Ethics Committee at the Institute of Information and Communication Sciences of the Bulgarian Academy of Sciences and has been applied in conducting experimental research for verification of a methodology for predicting consumer choice based on the integration of an EEG-based MMI and a social robot Furhat for intelligent marketing. The procedure defines the main goal of the study, the location of the electrodes on the scalp - in the prefrontal, fronto-central and parietal (parietal) areas and the main neural frequencies - theta (4–8 Hz), alpha (8-13 Hz), beta (13-30 Hz) and gamma (30-45 Hz). To assess whether the power of the EEG data corresponds to the results of existing research in the field of neuromarketing, it is necessary to calculate the average power of the signals from the electrodes AF3, AF4, F3, F4, F7, F8, FC5, FC6, Cz, Pz, P3 and P4 for the two separate states - "Like" and "Dislike". In the framework proposed in Chapter 3 for integrating the OpenBCI device with the social robot Furhat for conducting neuromarketing analyses, brain wave activity is recorded from the moment of visualization of the marketing product to the moment of selecting a response by the participant. To stimulate brain activity during the presentation of a marketing product, a web application was developed on a screen external to the Furhat robot, with the possible responses being "like", "dislike" and "buy". The obtained EEG activity in specific brain regions was analyzed based on previously studied scientific literature and neuroexpertise and compared with the participant's neural activity. The experimental study involved people of both sexes aged between 21 and 59 years. The criteria for selecting participants included interest in the experiment and lack of discomfort due to the placement of the OpenBCI cap with wet electrodes. The criterion for excluding participants was voluntary refusal after familiarization with the experimental procedure. Each participant was previously informed by the scientific supervisor about the objectives of the study, its methodology, duration, limitations and foreseeable risks. A summary of this information was provided in the consent form, which the participants signed in advance. The experimental procedure included processes for anonymization, archiving and protection of the data acquired during the experiment.

4.1.1 Experiment scenario and materials used and methods

For the purpose of this dissertation, an experimental setup (Fig. 27) was built to conduct an experimental study that uses a non-invasive, portable, EEG-based MMI device OpenBCI, which is open source and is designed to work with all OpenBCI boards. The boards used are Cyton OpenBCI, which is an 8-channel interface compatible with Arduino and is equipped with a 32-bit processor, and Daisy OpenBCI, which connects to Cyton OpenBCI, and together they allow recording of EEG signals from 16 channels. In the Cyton/Daisy configuration, data is collected at a frequency of 125 Hz on each of the 16 channels.

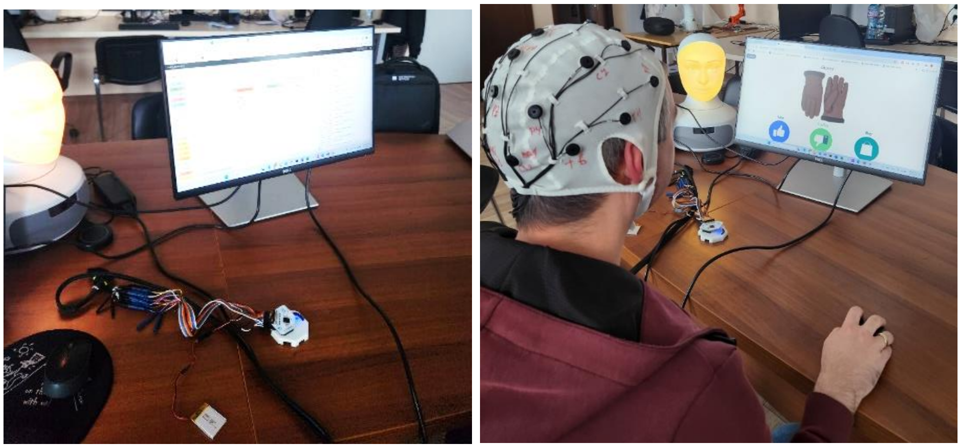

Fig.27 Experimental setup for conducting the experimental study

For the purposes of the experiment, communication flows were developed in the Node-RED platform, presented in detail in Chapter 3, using the previously developed library of input nodes openBCI toolkit (https://flows.nodered.org/collection/W7dKrufq2WWR). At the start of the experiment, the raw EEG data recorded by CytonDaisy are continuously recorded and sent wirelessly to a laptop with a running Node-RED server via Bluetooth. Initially, a web session is started to the BrainFlow server, which provides streaming transmission of the EEG data, after which they are stored in the global variables of Node-RED. At the start of the experiment, reference values for these electrodes and frequency bands are recorded in a static .csv file, after which each marketing stimulus is started. From the start of the marketing stimulus by visualization on the Furhat screen to the indication of a response by the participant, the values for the raw EEG signals are recorded by electrodes in a separate .csv file, after which they are filtered, normalized and transformed in the frequency domain. After extracting the characteristics of the EEG data, they are collected and processed into a single array for the purpose of analyzing the average neural activity between participants.

4.1.2 Participants

Experimental studies were conducted with 9 participants, with an average age of 33 years. Each participant was previously informed by the scientific supervisor about the objectives of the study, its methodology, duration, limitations, foreseeable risks and signed a consent form. Each participant was placed in front of a Furhat robot with a graphical interface device (React GUI) displaying a marketing survey of five marketing products or incentives (Fig. 30) with "endorsement" or "promotion", 15 in total. The participant was asked to choose, through the graphical interface, the spontaneous response "I like", "I dislike" or "I buy" for each of the products.

Fig. 30 Marketing products (stimuli)

A non-allergenic contact gel is required for the electrodes of the EEG device and is placed at the beginning of the experiment in the electrodes of the cap with each participant. Each participant is instructed that it is undesirable to swallow forcefully or move their head abruptly. Time is needed to place the device, to establish contact with the scalp and to determine the reference values of the frequency range. Of the total duration of the experiment (about 15 minutes), the actual experiment is about 5 minutes.

4.2 Development of a custom Python-based environment for EEG data analysis

In order to study the spontaneous emotional reactions of consumers to product advertising and their choices, it is necessary to process the registered raw EEG signals and discriminate them regarding the preferences of the participants. For this purpose, a customized Python-based environment has been developed for pre-processing, correlation and statistical analysis of the characteristics of EEG signals. In Appendix 3, the scripts are provided in order to ensure transparency and subsequent reproducibility in the processing, analysis and statistical interpretation of the results. The developed environment integrates several open Python libraries for conducting quantitative analyses on EEG data: pandas / numpy; scipy.signal (butter, filtfilt, savgol_filter, welch, find_peaks); scipy.stats (f_oneway, ttest_ind, pearsonr); dtaidistance.dtw; sklearn.metrics.pairwise.cosine_similarity.

4.3 Data processing and analysis

The raw EEG signals were preprocessed in Node-RED using a bandpass filter (0.5–40 Hz) to remove low-frequency deviations, muscle artifacts, and high-frequency electrical noise, and a notch filter was used to reduce interference from the power grid. After filtering, the EEG signals were normalized using z-score normalization to ensure comparability between channels for different participants. The normalization parameters were the mean (μ) and standard deviation (σ), which were calculated during the session from the first three intervals (each 5 seconds) between two “Until answer” blocks (during the Check Mark of the timeline in Fig. 31). The data were then segmented into stimulus-synchronized blocks by extracting EEG data between the beginning and end of the stimulus, and assigned behavioral labels “Like”, “Dislike”, and “Buy”. Each EEG data point x, normalized by a z-score according to the formula $y=(x-\mu)/\sigma$, has a value close to 0 when brain activity is close to the calibration mean; a value around ±1 corresponds to approximately one standard deviation from the mean; and a value around ±2 represents approximately two standard deviations from the mean. All stimulus-synchronized blocks are merged into a single data set to allow averaging and analysis across all participants..

Fig.31 Time order of stimuli in experimental research

As described in Chapter 3, stimuli are considered distinguishable when their dynamics across different frequencies and electrodes in sliding windows are weakly or negatively correlated: a high Pearson coefficient $r \geq -0.6$ defines uncorrelated dynamics, and a negative coefficient indicates a significant difference in the geometry of the temporal profiles of the neuromarker in sliding windows. A threshold of $r \geq -0.6$ was chosen based on scientific evidence. For cosine similarity, a threshold ≥ -0.5 (corresponding to an angle < 60°) was chosen (Table 1). Due to the lower computational complexity, only the results of the Pearson correlation for "Like" versus "Dislike" decisions were analyzed.

Table 1. Comparison of Pearson correlation and cosine similarity of the second derivative of the spectral power of the frequencies in the different electrodes in the interval (0.5–2.0 s), for which negatively correlated dynamics to the different stimuli are observed

Band	**Inverse channels**		**Weak channels (first 3)**	
	Pearson r ≤ -0.6	**Cosine ≤ -0.5**	**Pearson r**	**Cosine**
Theta (4-8 Hz)	AF3:-0.975 F3:-0.934 C3:-0.870 AF4:-0.810 Pz:-0.743 P4:-0.697	F3:-0.802 AF3:-0.78 F8:-0.726 P4:-0.646 C3:-0.636 T7:-0.624 T8: -0.623	T8:-0.557 T7:-0.527 F7: -0.289	Pz:-0.27 AF4: -0.09 F4: 0.105
Alpha (8-13 Hz)	C3: -0.959 F8: -0.959 P3: -0.929 F3: -0.830 AF4:-0.783 C4: -0.697	C3:-0.912 F8:-0.784 Cz:-0.692 F3: -0.641 AF4:-0.56	P4: -0.183 AF3:-0.17 O1: 0.347	P3:-0.37 C4:-0.022 AF3: 0.131
Beta (13-30 Hz)	AF4:-0.693	O1: -0.737 AF4: -0.617	O1: -0.598 F3: -0.496 P4: -0.391	T7:-0.422 F3:-0.342 F7:-0.121
Gamma (30-100 Hz)	O2: -0.693	O2: -0.572	O1: -0.489 Cz: -0.453 F4: -0.356	C3:-0.492 Cz: -0.480 F4: -0.407

4.3.1 Similarity in the shape of the second derivative of spectral power curves between "Like" and "Dislike" responses

A comparison of the average spatiotemporal EEG dynamics for the "Like" and "Dislike" choices was made for the acceleration of the EEG signal power in the theta, alpha, beta and gamma frequency bands using equation (1). Electrodes showing strong inverse correlations (r ≥ -0.6) were interpreted as important neuromarkers for spontaneous consumer choices.

Theta band (4–8 Hz)

In the theta band, electrodes showing strong inverse correlations (r ≥ -0.6) for the neuromarkers of the two choices "Like" and "Dislike" in sliding windows of 0.25 ms are observed primarily in the prefrontal, frontal and parietal regions (Figure 32) - AF3, F3, C3, AF4, Pz and P4.

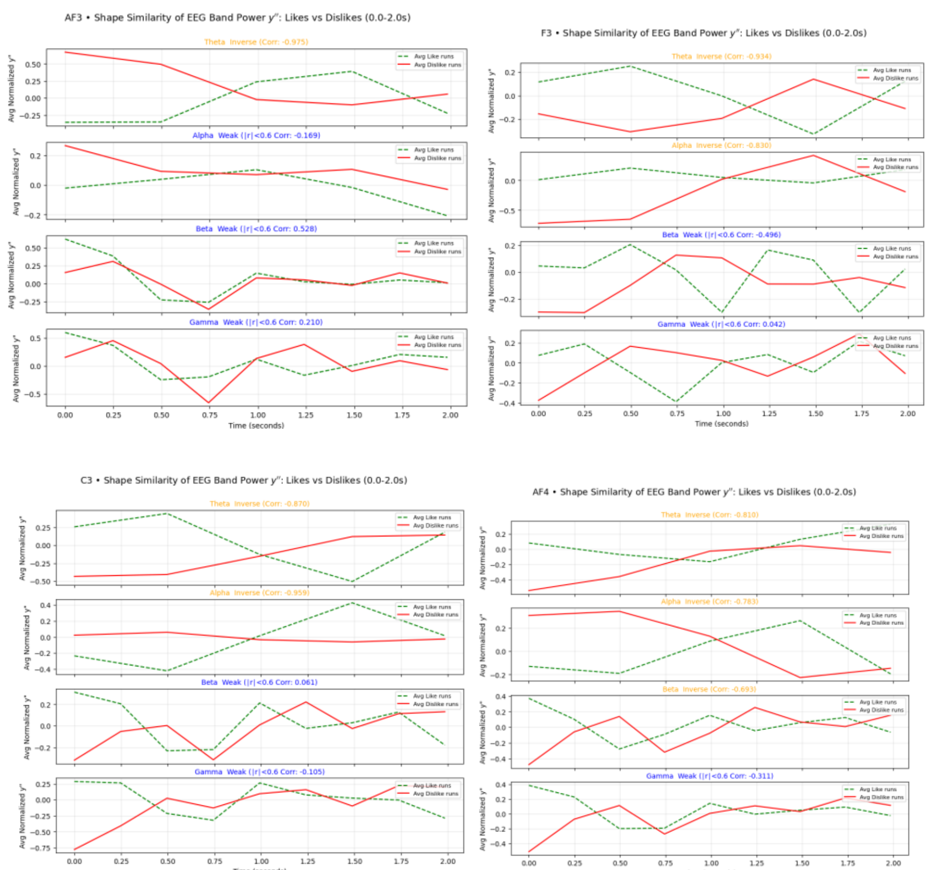

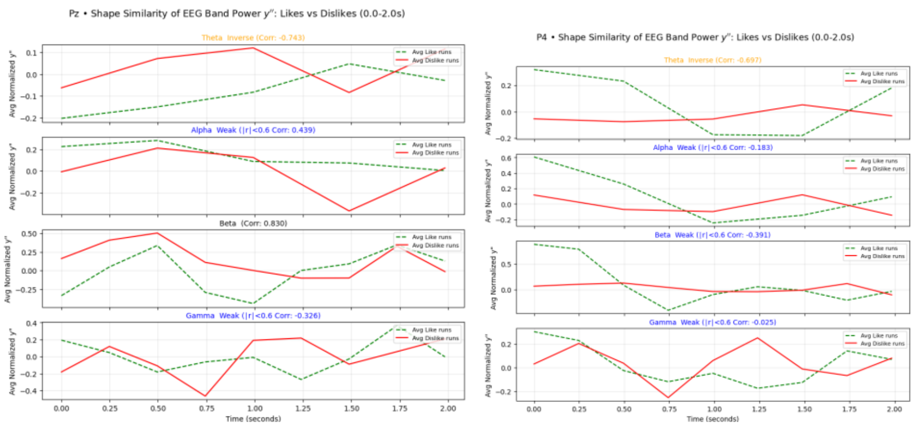

Fig.32 The greatest difference in the shape of the second derivative of theta power curves between "Like" and "Dislike" responses is observed at electrodes AF3, F3, C3, AF4, Pz and P4.

A great similarity in the shape of the curves is observed at the central and occipital electrodes Cz, O1, O2, P3, suggesting that both stimuli evoke similar neuronal activity around the central part of the brain.

Alpha band (8–12 Hz)

The electrodes showing strong negative correlations in the geometric shape of the spectral power acceleration for the two sliding window choices are: C3, F8, P3, F3, AF4 and C4 (Fig. 32), and the values can be seen in Table 1. A great similarity in the shape of the curves is observed in the temporal, occipital and central regions for electrodes T7, O2, Cz and T8.

Beta band (13-30 Hz)

There is a great similarity in the shape of the curves for the two choices at the beta frequency, especially in the central and parietal regions: electrodes Cz, Pz, C4, T8 and P3. Only electrode AF4 shows a strong negative correlation in the geometric shape of the acceleration of the spectral power in sliding windows (Figure 32).

Gamma band (30-40 Hz)

There is a great similarity in the shape of the curves for the two choices at the theta frequency, with only the O2 electrode showing a strong negative correlation..

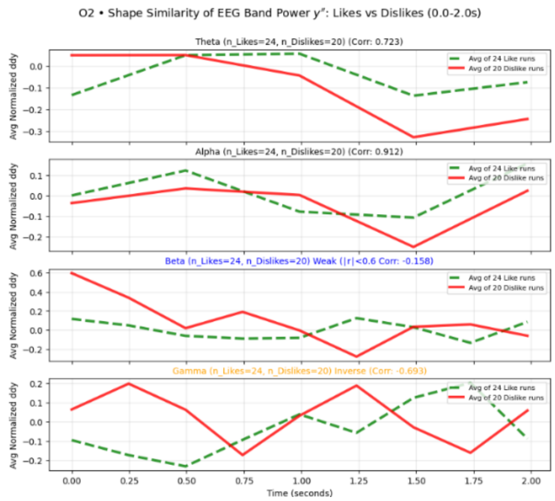

Фиг.33 Shape of the second derivative of the frequency power curves between “Like” and “Dislike” responses for O2 electrode

4.3.2 Cohen's d coefficient and 95% confidence interval between "Like" and "Dislike" responses

A measure of the magnitude and direction of the effect at the distribution level was applied by calculating Cohen's d coefficient according to formula (3) and the corresponding 95% confidence intervals according to formula (5) for the “Like” versus “Dislike” conditions for all electrodes and frequency bands within the first 2 seconds after the stimulus appeared on the screen. In contrast to the Pearson correlation, which quantifies the similarity or difference in the geometry of the temporal-spatial profiles of the neuromarker in sliding windows, but does not measure the differences between the mean values of the conditions, the variability within a given condition and the dispersion between individual participants and trials. In order to account for these characteristics at the distribution level, Cohen's d coefficient was also integrated into the dynamic analysis with the corresponding 95% confidence intervals for the different experimental conditions. As a result of this integration, the resulting representation of the similarity between channels is presented in Table 2.

Table 2: A summarized representation of similarity between electrodes, where the greatest significance is determined by combining statistically significant Pearson correlations and effect sizes whose 95% confidence intervals do not include zero.

Band	Type of Evidence	Channels	Effect Sizes |d| ≥ 0.60 and 95% CI excludes 0
Theta (Overlap 83%)	Pearson correlation only	C3	-
	Effect only	F8, T8, Cz, F7, T7	F8: 1.27 (0.62–1.92); T8: 1.11 (0.47–1.75); Cz: 0.84 (0.22–1.46); F7: 0.73 (0.12–1.34); T7: –0.66 (–1.27 to –0.06)
	Consolidation	AF3, F3, AF4, Pz, P4	AF3: –0.81 (–1.43 to –0.19); F3: 0.81 (0.19–1.42); AF4: 1.10 (0.46–1.73); Pz: –1.17 (–1.82 to –0.53); P4: 0.63 (0.03–1.24)
Alpha (Overlap ≈ 33%)	Pearson correlation only	P3, C3, F8, AF4, C4, Cz, O2, O1	-
	Effect only	AF3, F7	AF3: –1.09 (–1.73 to –0.46); F7: 0.61 (0.00–1.22)
	Consolidation	F3, Pz, T8, T7	F3: 0.89 (0.27–1.51); Pz: 0.77 (0.16–1.39); T8: 0.65 (0.04–1.26); T7: –0.61 (–1.22 to –0.01)
Beta (Overlap 50%)	Pearson only	P3, AF4	-
	Effect only	T7	–0.64 (–1.25 to –0.03)
	Consolidation	Cz, Pz	Cz: –0.65 (–1.26 to –0.04); Pz: –0.61 (–1.22 to –0.01)

The strongest Cohen effects appear in the theta band, where several electrodes show large and statistically reliable differences between conditions. Electrode F8 dominates with a "Like" response (d=1.27, 95% confidence interval fully above zero), followed by electrodes T8 (d=1.11) and AF4 (d=1.10), both of which reflect strong activity for "Like" responses in right temporal and frontal regions. In contrast, Pz shows a strong "Dislike" dominant pattern (d=-1.17, 95% confidence interval fully below zero), indicating reliable parietal differentiation. In the alpha band, AF3 demonstrates a clear "Dislike" dominant effect (d=-1.09, 95% confidence interval fully negative), highlighting the suppression of the left frontal region during "Like" responses.

4.3.3 Similarity in the shape of the second derivative of spectral power curves for "Buy" responses between "promotion" and "endorsement" stimuli

It is important to note that among all participants, only four purchase cases were registered in the "discount" condition and three in the "product placement" condition. Therefore, the results require confirmation through additional experiments with a larger set of baseline EEG data..

Theta band (4-8 Hz)

The strongest discriminating effects between the "promotion" and "product placement" stimuli were observed outside the frontal brain area. Very strong inverse patterns were observed in O2 (r=-0.935), O1 (r=-0.887) and Cz (r=-0.837), suggesting oppositely structured theta-band dynamics across conditions. These effects are consistent with differential visual-attentional processing in occipital regions (O1/O2) and different processes related to decision-making or action preparation reflected in the midline (Cz). In contrast, frontal electrodes showed weak or very similar theta dynamics across conditions.

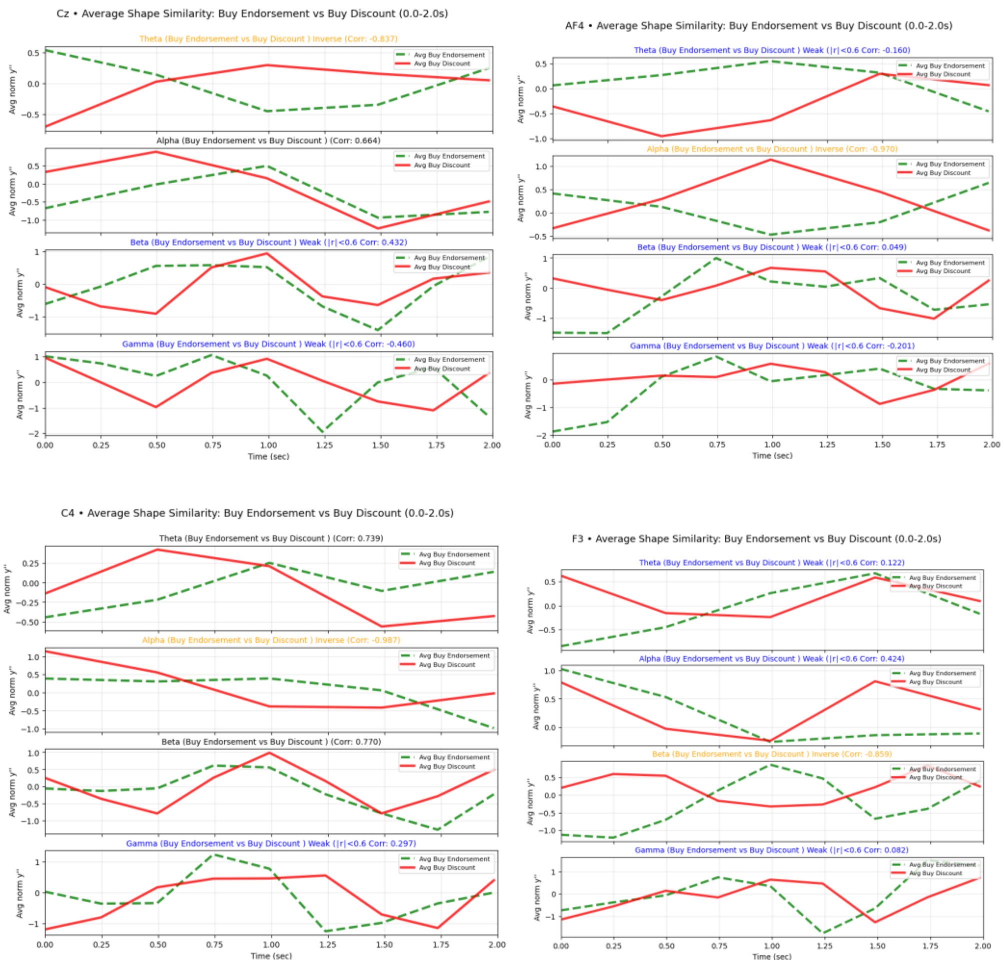

Fig.35 The largest weakly or negatively correlated dynamics for "Buy" (product positioning vs. discount) are observed at electrodes O2, O1 and Cz for theta, AF4 and C4 for alpha, O2, F3 and P3 for beta and Pz, F4 and O1 for gamma frequencies

Alpha band (8-12 Hz)

The largest negatively correlated dynamics for alpha frequency were observed in C4 (r = -0.987) and AF4 (r = -0.97). These results indicate a strong right hemisphere dominance, reflecting differences in frontal inhibitory control and cognitive evaluation between the "endorsement" and "after discount" conditions..

Beta band (13-30 Hz)

The largest negatively correlated dynamics for beta frequency were observed in O2 (r = -0.917), F3 (r = -0.859) and P3 (r = -0.732). The obtained results suggest the presence of condition-specific differences related to confidence in visual decision-making and control of executive functions in the left frontal region.

Gamma band (30-40 Hz)

The largest negatively correlated dynamics for theta frequency were observed in Pz (r = -0.836), F4 (r = -0.784) and O1 (r = -0.644). These results indicate that gamma activity in the right frontal cortex exhibits increased sensitivity to socially conditioned, compared to price-conditioned, motivational processes. This is consistent with the established role of the posterior parietal lobe in the mechanisms of attentional guidance and behavioral regulation in decision-making.

4.3.4 Cohen's d coefficient and 95% confidence interval between the terms "promotion" and "endorsement"

Due to the small number of "Buy" responses, no distribution-level analysis was applied for the size and direction of the effect when comparing averaged responses for "Buy".

4.4 Discussion of the results

The proposed analysis is based on the second derivative of spectral power (P) in different frequency bands, which allows to capture the dynamics of EEG signals and to reveal spatiotemporal structures invisible in the original signals of the rate of change of EEG power in sliding windows for each frequency band and channel ($y'' = d^2P/dt^2$) for spontaneous responses (0.5–2.0 s) to different stimuli. Electrodes and frequency bands with inversely correlated similarity in the shape of d^2P/dt^2 curves between different choices are significant. The obtained results show that neuromarketing-related EEG differences are mainly in the spatiotemporal dynamics of brain activity, and not in the static characteristics of absolute or relative power. The observed inverse dynamics indicate that impulsive decisions "like" and "dislike" engage oppositely structured transitions of neural states and therefore can serve as a neuromarker for dynamic, stimulus-based discrimination. Furthermore, in neuromarketing, social robots could serve as interactive interfaces to BCI systems, helping to overcome the main challenge of EEGs, namely how they are interpreted, by providing explanations and real-time feedback while predicting consumer choices.

4.4.1 Discriminative EEG spatiotemporal dynamics underlying "Like" and "Dislike" responses

Table 1 presents the most significant electrodes and frequencies where the second derivative of spectral power (P) curves are negatively correlated for the choices "Like" and "Dislike". In the theta frequency, these are electrodes AF3 (-0.975) and F3 (-0.934), in the alpha band - C3 (-0.959), F8 (-0.959) and P3 (-0.929). Overall, the theta and alpha bands are the strongest discriminators, showing the largest number of significant channels (6 out of 16), indicating strongly polarized spatiotemporal dynamics between conditions. The observed theta patterns in the data, especially in the prefrontal and frontal electrodes F3, AF3 and F8, which mark modulation by negative or aversive stimuli and engagement of cognitive control by negative outcomes. Regarding alpha activity, the results show that emotional valence modulates alpha activity, with the strongest effects observed in the centro-parietal regions (C3: -0.959; P3: -0.929), followed by the frontal regions (F8: -0.959; F3: -0.830; AF4: -0.783). Regarding beta activity, the strongest discriminative inverse patterns were observed in electrode O1, associated with emotional visual processing, and AF4 (right frontal lobe), associated with emotional/cognitive conflict and avoidance tendencies.

Based on the derivative-based shape similarity analysis and the statistical analysis of effect size, electrodes AF3, F3, AF4, Pz, and P4 were identified as the most stable theta electrodes, with an inverse shape. All five electrodes demonstrated both structural temporal dynamics and statistically reliable mean separation, with confidence intervals excluding zero. Effect sizes were large for AF3 ($d = -0.81$, 95% CI: -1.43 to –0.19), F3 ($d = 0.81$, 95% CI: 0.19-1.42), AF4 ($d = 1.10$, 95% CI: 0.46-1.73) and Pz ($d = -1.17$, 95% CI: -1.82 to -0.53), while P4 showed a moderate but reliable effect ($d = 0.63$, 95% CI: 0.03–1.24).

4.4.2 Discriminative EEG spatiotemporal dynamics underlying purchase decisions based on discounts and product positioning

The distinction between purchase decisions based on discount and those based on product placement is particularly evident in gamma activity in the right frontal and occipital regions associated with attentional dynamics. These patterns suggest that the two decision contexts engage different motivational and evaluative strategies, rather than simply differing in stimulus intensity. Again, the limitation of comparing averaged responses for the “Buy” conditions is noted, as the sample contained only seven purchase events in total, making statistical generalization difficult. Strong discrimination was observed between the product placement and discount conditions, reflected in inverse-shaped patterns observed for theta at electrodes O2, O1, Cz, and alpha with a coefficient of $r\sim-0.98$ at C4 and AF4. Comparison of purchase decisions based on product positioning and discount-based decisions revealed significant differences in neural dynamics, especially in the occipital region—electrodes O1/O2 (Figure 30). In theta frequency, product positioning and discount choices followed inversely correlated curves, suggesting differential engagement of cognitive control and evaluative processes. Theta activity is typically associated with decision-making and conflict monitoring; therefore, negatively correlated dynamics in product positioning-based decisions indicate internal activation of evaluative mechanisms (e.g., trust, social validation), while discount-based decisions engage external activation based on stimulus processing. Similarly, alpha frequency activity in electrodes C4 and AF4 showed a strong inverse relationship between conditions. In the beta frequency, clear discrimination between conditions was observed, with strong inverse correlations at electrodes O2 ($r = -0.917$), F3 ($r = -0.859$) and P3 ($r = -0.732$). Beta activity in the occipital and parietal regions is associated with visual processing of displayed stimuli and decision-making confidence, while beta activity in the left frontal region is usually associated with cognitive control. In the gamma frequency, negatively correlated dynamics were found at Pz ($r = -0.836$), F4 ($r = -0.784$) and O1 ($r = -0.644$). Compared with the scientific literature, these results indicate that the dynamics of the gamma range are sensitive to differences between social and price-related motivational processes, which is consistent with the established role of fronto-parietal neural circuits in directing attention and decision-making behavior. In the context of neuromarketing, it is known that decisions based on product positioning tap into social influence and affective processing systems, a finding that has been consistently reported in EEG neuromarketing studies. Systematic reviews of EEG neuromarketing research have shown that emotionally and socially charged messages reliably modulate frontal EEG markers and predict preferences and purchase intention. EEG experiments comparing human and virtual test subjects demonstrate that endorsement contexts alter both behavioral purchase intentions and neural activity, providing empirical evidence that endorsement cues activate evaluation processes at the neural level.

Conclusions on chapter 4

A social robot for marketing purposes has been successfully implemented, which verbally and visually presents products with three possible choices ("Like", "Dislike", "Buy"). The conducted research shows that the use of a social robot leads to longer attention retention and increased engagement of participants, which creates conditions for more reliable registration and analysis of EEG signals in BCI-based marketing.

The novel neuromarker developed in Chapter 3, based on spatiotemporal analysis of the similarity of the second derivative in sliding windows, was applied to compare brain activity for a given choice. In the interval 0.5-2 sec. after the stimulus, a strong neuronal differentiation was observed, expressed by Pearson's inverse correlations ($r < -0.60$), strongest in the theta band at electrodes AF3, F3, C3, AF4, Pz and P4, with additional effects in the alpha, beta and gamma ranges.

The statistical evaluation based on the effect size, by calculating Cohen's d coefficient with 95% confidence intervals for the stimuli "like" versus "dislike", identified the proposed neuromarker as reliable, after applying the criterion $|d| \geq 0.60$ with confidence intervals excluding zero. After summarizing the dynamic and statistical results, it was found that the effects were most pronounced primarily in the front and central theta-band electrodes AF3, F3, AF4, Pz and P4, with additional effects in the alpha band at electrodes F3, Pz, T7 and T8, as well as in the beta band at electrodes Cz and Pz.

The results are compared with neuromarketing studies reported in the scientific literature and show that the proposed novel neuromarker is computationally efficient and statistically reliable for use by robotic systems integrated with MMI to decode impulsive buying reactions in consumers.

Directions for future research

In the proposed method for analyzing EEG data, the values collected from the electrodes of interest are processed post hoc. The method for analyzing EEG data in real time based on the novel neuromarker and analyzing the similarity of spontaneous neuro-responses using the Pearson coefficient is to be applied in order to predict the momentary preference of users.

Due to the small number of "Buy" responses, a full statistical summary cannot be made. The distinction between purchase decisions based on discount and those based on product positioning needs to be re-verified through a new experimental study with a larger number of participants..

Contributions of the dissertation

1. A novel conceptual model for interaction with social robots via EEG signals in an IoT environment has been developed, implemented using the Node-RED platform. The main functional requirements for transmission, analysis and processing of EEG signals and their conversion into control commands for social robots have been formulated..

2. Original methods and algorithms have been developed to easily transform social robots into IoT devices - for Pepper via MQTT and Python child processes in Node-RED, and for Furhat via HTTP protocol with GET/POST requests from the behavior management software module, processed in Node-RED by an HTTP receiving node.
3. An IoT-based architecture for the integration of EEG-based MMI and social robots has been developed, implemented in Node-RED with ready-made nodes for EEG devices and visual programming, which, by executing external Python child processes, provides dynamic management of hardware and software resources and asynchronous data exchange.
4. In the field of neuromarketing, novel methods and algorithms have been developed for analyzing the dynamic similarity of spatiotemporal EEG signals reflecting the spontaneous reactions of users, by extracting features based on the second derivatives of the power of the signals.
5. Based on these algorithms, a novel neuromarker for assessing consumer choice using Pearson correlation in sliding windows is defined. It measures the spatiotemporal similarity of responses (up to ~2 sec.) and offers a computationally lighter alternative to classical wavelet analysis and Fourier transform.
6. A novel methodology and software for real-time neuromarketing research have been developed and experimentally verified by integrating OpenBCI and the social robot Furhat. By combining dynamic similarity analysis in sliding windows and statistical analysis (Cohen’s d with 95% confidence intervals), the key electrodes and frequency bands reflecting spontaneous emotional reactions to consumer choices have been identified..

List of publications

[1]. **S. E. Kremenski** and A. K. Lekova, "Brain-robot Communications in the Internet of Things," 2022 International Conference on Information Technologies (InfoTech), Varna, Bulgaria, 2022, pp. 1-6, doi: 10.1109/InfoTech55606.2022.9897117 SJR(Scopus) =0,147

[2]. Kremenska, Adelina & Lekova, Anna & **Kremenski, Svetoslav** & Dimitrov, Georgi. (2025). Validating the openBCI Nodes through EEG-based BCI Application for Smart Home Automation Control. Journal of Communications Software and Systems. 21. 250-261. 10.24138/jcomss-2025-0012. IF (WoS): 0.7 Q3

[3]. **Svetoslav Kremenski**, Anna Lekova, Adelina Kremenska, A BCI Framework Using Derivative Similarity Metrics to Characterize EEG Spatiotemporal Dynamics with Applications in Neuromarketing, WSEAS TRANSACTIONS on SIGNAL PROCESSING (in print - Paper ID: eeacs2026-114)

Noted citations

1. Weike, Michel & Ruske, Kai & Gerndt, Reinhard & Doernbach, Tobias. (2024). Enabling Untrained Users to Shape Real-World Robot Behavior Using an Intuitive Visual Programming Tool in Human-Robot Interaction Scenarios. 10.1145/3648536.3648541.
2. Bal, Fatma & Tekerek, Mehmet & Gök, Mehmet & Şimşir, Ramazan & Palacz, Magdalena. (2024). Human Robot Interaction with Social Humanoid Robots. El-Cezeri Fen ve Mühendislik Dergisi. 11. 94-102. 10.31202/ecjse.1390219.
3. Zhang, Y., Rajabi, N., Taleb, F., Matviienko, A., Ma, Y., Bjorkman, M., & Kragic, D. (2024). Mind Meets Robots: A Review of EEG-Based Brain-Robot Interaction Systems. ArXiv, abs/2403.06186.
4. Marinho, I. N. (2024). Brain Controlled UGV: Desenvolvimento de veículo terrestre não-tripulado controlado por interface cérebro-computador
5. Rakhmatulin, I., Naik, G.R. (2026). Case Studies and Applications. In: EEG Signal Processing with Python. Brain Informatics and Health. Springer, Singapore. https://doi.org/10.1007/978-981-95-4177-5_14

ACKNOWLEDGEMENTS

With deepest gratitude, I would like to express my gratitude to all those who stood by me and encouraged me during the years of working on my doctoral dissertation. I have made it this far thanks to the support of my supervisors, colleagues, family and friends.

I want to express my sincere gratitude to my supervisor Prof. Dr. Anna Lekova, who has always encouraged and helped me with her professional skills, competence and creativity. Without her assistance and valuable guidance, the completion of this dissertation would not have been possible. My personal admiration for her scientifically and socially significant work is undoubtedly the reason why I did not give up, but rather overcame the challenges I encountered.

I express my sincere gratitude to my second supervisor, Prof. Dr. Snezhanka Kostova, whose collaboration made this dissertation possible..

I also express my gratitude to my colleagues from the IRCS section and the Institute of Robotics at the Bulgarian Academy of Sciences for their assistance and responsiveness.